NASA CR-120786
Final Report: 1754-1

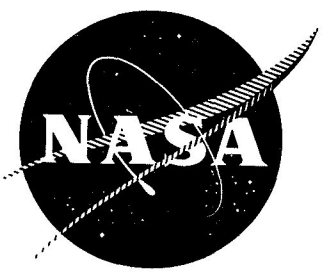

MEASUREMENT OF THE VISCOSITY BY THE OSCILLATING CRYSTAL METHOD OF FOUR FLUIDS AS FUNCTIONS OF PRESSURE, SHEAR RATE AND TEMPERATURE

by R. G. Rein, T. T. Charng, C. M. Sliepcevich, and W. J. Ewbank

THE UNIVERSITY OF OKLAHOMA RESEARCH INSTITUTE

prepared for

NATIONAL AERONAUTICS AND SPACE ADMINISTRATION

NASA Lewis Research Center
Contract NAS 3-13487

1. Report No.	2. Government Accession No.	3. Recipient's Catalog No.
NASA CR-120786		

4. Title and Subtitle	5. Report Date
MEASUREMENT OF THE VISCOSITY BY THE OSCILLATING CRYSTAL METHOD OF FOUR FLUIDS AS FUNCTIONS OF PRESSURE, SHEAR RATE AND TEMPERATURE	September 1, 1971
	6. Performing Organization Code
7. Author(s) R. G. Rein, T. T. Charng, C. M. Sliepcevich, and W. J. Ewbank	8. Performing Organization Report No. Final Report: 1754-1
	10. Work Unit No.
9. Performing Organization Name and Address The University of Oklahoma Research Institute Norman, Oklahoma 73069	11. Contract or Grant No. NAS 3-13487
	13. Type of Report and Period Covered Contractor Report
12. Sponsoring Agency Name and Address National Aeronautics and Space Administration Washington, D.C. 20546	14. Sponsoring Agency Code

15. Supplementary Notes

Project Manager, William R. Loomis, Fluid System Components Division, NASA Lewis Research Center, Cleveland, Ohio

16. Abstract

Measurements of the viscosity of four synthetic lubricating fluids (Mobil XRM-109F, DuPont Krytox 143-AB, Humble FN-3158, and Humble FN-3158 plus ten volume percent of Kendall 0839) were made at temperatures to 300° F and pressures to 40 000 psig with an oscillating quartz crystal viscometer. Viscoelastic behavior of two of the test fluids (Mobil XRM-109F and Humble FN-3158 plus ten volume percent of Kendall 0839) was indicated at 100° F and elevated pressures, but current limitations in the experimental apparatus precluded further investigation of this phenomenon. However, in order to demonstrate the techniques, the viscoelastic behavior of one of the calibration fluids, di- (2-ethylhexyl) sebacate, was determined. These data were then used to compute the reduced elastic (storage) modulus and the shear relaxation spectrum as functions of reduced frequency. In addition, the effect of pressure and temperature on the density of the four test fluids was measured.

17. Key Words (Suggested by Author(s))	18. Distribution Statement
Oscillating quartz crystal; Viscometer; Viscoelastic behavior; Elastic modulus; Shear relaxation spectrum; Resonant frequency; Non-Newtonian behavior; Reduced variables	Unclassified - unlimited

19. Security Classif. (of this report)	20. Security Classif. (of this page)	21. No. of Pages	22. Price*
Unclassified	Unclassified	65	$3.00

* For sale by the National Technical Information Service, Springfield, Virginia 22151

ACKNOWLEDGMENTS

A number of individuals provided valuable assistance during the course of this project, particularly:

Professor Gerald Tuma of the School of Electrical Engineering for his advice on electronics and instrumentation.

Professor Robert Block and Mr. Steve Conner of the School of Materials Science for plating the silver electrodes on the crystals.

The John Roberts Company of Norman, Oklahoma, for drilling the quartz crystals.

The Rohm and Haas Company for supplying the di-(2-ethylhexyl) sebacate.

Professor Craig Jerner of the School of Materials Science for his metallurgical analysis of a failure in the closure for the high pressure cell.

Mr. Gene Scott of the Physics Instrument Shop for his suggestions and machining of replacement parts in the high pressure system which proved to be superior to the original components.

Dr. Hossein Nouri for his viscosity measurements on the four test fluids using a Cannon-Fenske viscometer at atmospheric pressure.

TABLE OF CONTENTS

FINAL REPORT ON

MEASUREMENT OF THE VISCOSITY BY THE OSCILLATING CRYSTAL METHOD OF FOUR FLUIDS AS FUNCTIONS OF PRESSURE, SHEAR RATE AND TEMPERATURE

by R. G. Rein, T. T. Charng, C. M. Sliepcevich, and W. J. Ewbank
UNIVERSITY OF OKLAHOMA RESEARCH INSTITUTE

INTRODUCTION

This report summarizes the work performed under Contract No. NAS 3-13487. The viscosities of four fluids supplied by NASA were measured over a range of pressures and temperatures using an oscillating quartz crystal method as described by Rein, et al. (13). The four fluids supplied by NASA were:

1. Mobil XRM-109F, a synthetic paraffinic hydrocarbon.
2. DuPont Krytox 143-AB, a perfluorinated polymer.
3. Humble FN-3158, a super-refined naphthenic mineral oil.
4. Humble FN-3158 fluid plus ten percent volume of Kendall 0839 super-refined paraffinic heavy resin.

The following test conditions were specified for each fluid:

1. At a constant temperature of 100°F and a constant pressure of 10,000 psig using crystal frequencies of about 20 kHz and 60 kHz.
2. At a constant crystal frequency of about 20 kHz and at pressures of 0, 10,000, 20,000, 40,000, 60,000, 80,000, 100,000 and 115,000 psig at constant temperatures of 100, 210 and 300°F and 250°C (482°F).

The current limitations on equipment restricted the measurements of viscosity on the four test fluids to a pressure of 40,000 psig and to a temperature of 300°F. However, it should be noted that density measurements were made up to 482°F and pressures to 115,000 psig with the calibration fluid di-(2-ethylhexyl) sebacate, which demonstrates that the present equipment is operable over the full temperature and pressure range originally sought but not for very viscous (above 10 poise) fluids without equipment modifications.

The following sections in this report include a description of the experimental techniques, the results in graphical form and tabulated experimental data in Appendices A and B, conclusions, experimental limitations and recommendations.

EXPERIMENTAL TECHNIQUES

The measurement of viscosity of fluids as a function of pressure has been reported by a number of investigators, but the most comprehensive and probably best known early studies are those of Bridgman (5) on pure compounds and the ASME Pressure-Viscosity Report (2) on lubricating oils. In both instances a falling-weight technique was used in which the shear rates were far too low to detect non-Newtonian behavior. Most of the published experimental work to date on viscoelastic behavior of fluids has been at atmospheric pressure.

The first significant studies on non-Newtonian behavior of fluids (polymer solutions) at high pressures (to 1000 atmospheres), at different temperatures (25 to 55°C) and high shear rates were those of Appeldoorn, et al (1) and Philippoff (11). They employed the principle of the oscillating quartz crystal viscometer introduced by Mason (10). More recently, Rein (13, 14) extended the techniques used by Philippoff to develop a viscometer for pressures to 8000 atmospheres. Rein subsequently redesigned the entire apparatus to permit viscosity measurements to pressures approaching 15,000 atmospheres and temperatures to 250°C and reduced shear rates on the order of 10^8 sec^{-1}. In addition, the effect of pressure and temperature on the density of the fluids can also be measured.

Experimental Equipment

A flow diagram for the experimental equipment is shown in Figure 1.

The high pressure cell, of shrink-fit duplex construction with an 18 percent nickel maraging steel inner liner and an HY-140 outer shell, was designed conservatively for use at 200,000 psi and 450°F. The quartz crystal was mounted on the

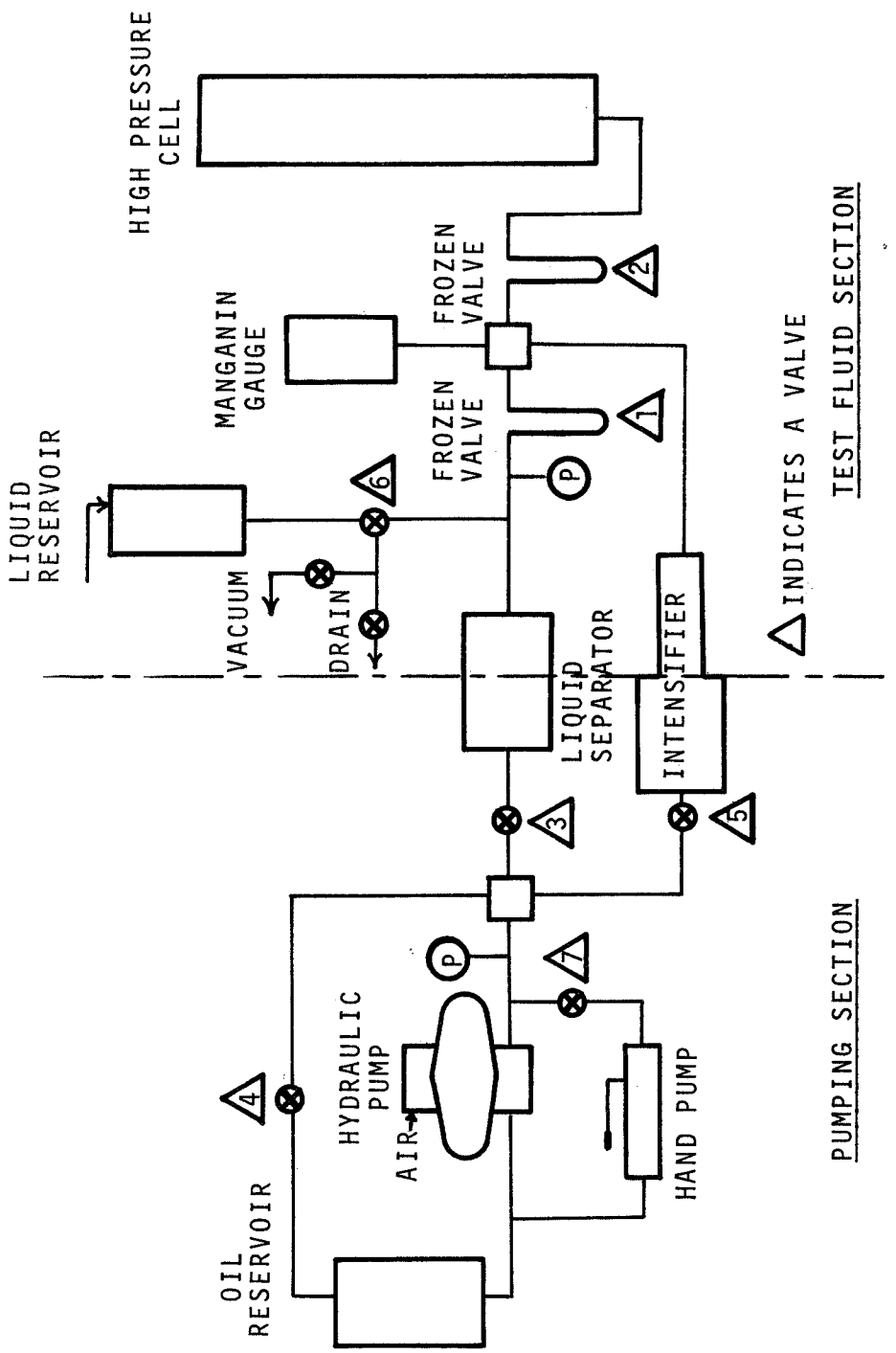

Figure 1. Flow Diagram of High Pressure Equipment and Accessories.

inside of the top closure and was connected to two electrical leads which entered through steel-pipestone conical-shaped plugs in the top closure.

A cell containing a coil of manganin wire (the change in resistance of the wire is a well-known function of pressure) was used for pressure measurements. The resistance of the manganin wire was measured with a Carey-Foster bridge. It is estimated that this combination measures pressures with an accuracy of better than ± 1/2 percent for pressures greater than 10,000 psi.

A sheath thermocouple entered the cell through the bottom closure. It was intended to use this thermocouple to measure the fluid temperature inside the high pressure cell. However, this thermocouple failed to operate midway through the test program; subsequently temperatures measured with a thermocouple on the cell wall consistently agreed with the temperature of the fluid in the cell to within ± 1/2°F after a 15 minute time interval, based on previous observations.

The temperature of the high pressure cell was maintained by immersing the cell in an oil bath which was heated by an electric heater. Temperatures of the fluid inside the cell were maintained to ± one percent.

An intensifier was used to pressurize the cell. The intensifier could be recycled by appropriate use of valves 1 and 2, shown in Figure 1, in order to attain the desired pressure in the cell. The principal disadvantage of this repetitive recycling is that it accelerates the wear in the packing and the fatigue life of the metal components.

The intensifier was constructed so that the advancing piston forces oil from the low pressure side, at the juncture between the low- and high-pressure pistons, into a sight glass as shown in Figure 2. Measurement of the amount of oil displaced was converted into piston travel for calculation of the densities of the test fluid in the high pressure side. The sight gauge was calibrated in 1/8 inch increments which provided sufficient

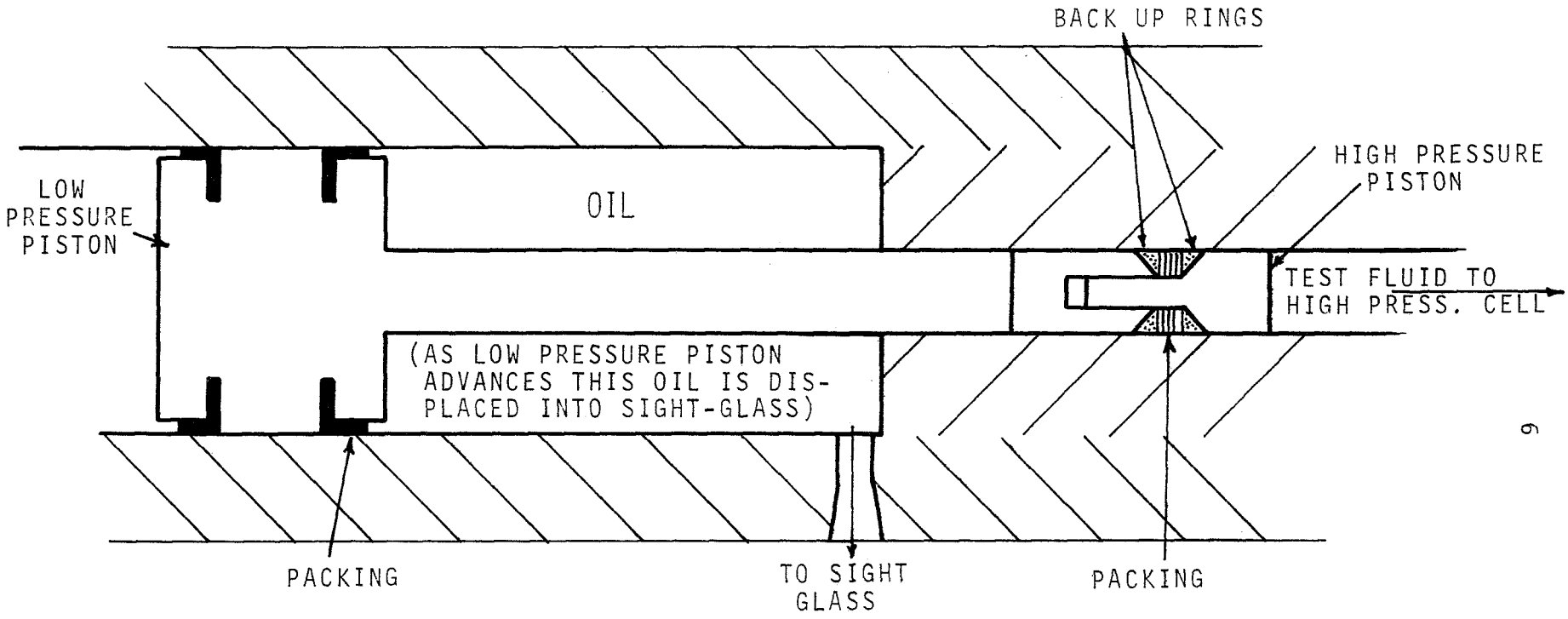

Figure 2. Schematic Diagram of Intensifier.

sensitivity to allow density measurements to be made within ± one percent, as confirmed by calibrations with di-(2-ethylhexyl) sebacate for which density determinations had been reported previously (2).

A liquid separator containing a piston and O-rings prevented communication of the fluid being tested with the hydraulic oil in the pumping section.

Valves 1 and 2, identified in Figure 1, consist of a section of U-shaped tubing which can be immersed in liquid nitrogen to freeze the test fluid; for this reason they are referred to as frozen valves. They were introduced by Babb (3), and they have proved to be absolutely leak-proof.

Figure 3 shows the electronic components used to measure the resistance of the oscillating quartz crystal as a function of frequency for each viscosity data point.

A prime requirement for the oscillator is high stability. The manufacturer specifies less than 0.003 percent drift in 10 minutes after warmup for this particular oscillator, which is adequate since the frequency will not change significantly during any measurement.

This particular impedance bridge has the advantage that the undesirable shunt effect of long cables is eliminated by the bridge design. The manufacturer claims an accuracy of at least ± one percent for resistance measurements with the bridge, and this accuracy can be generally attained. However, an accuracy of ± 5 percent at the high end of the dial seems more reasonable because of difficulty in reading it precisely at the high end.

Precision is the most important requirement for the counter used to determine the frequency of crystal oscillation because the calculated viscosities depend on a difference between frequency measurements. For fluids with low viscosities, such as lubricants at high temperatures, the resonant frequency in the test fluid differs from f_o, the resonant frequency in an inviscid fluid, by a small amount, 10-20 Hz. Therefore, if a counting or gate time of 10 seconds is used, the resulting

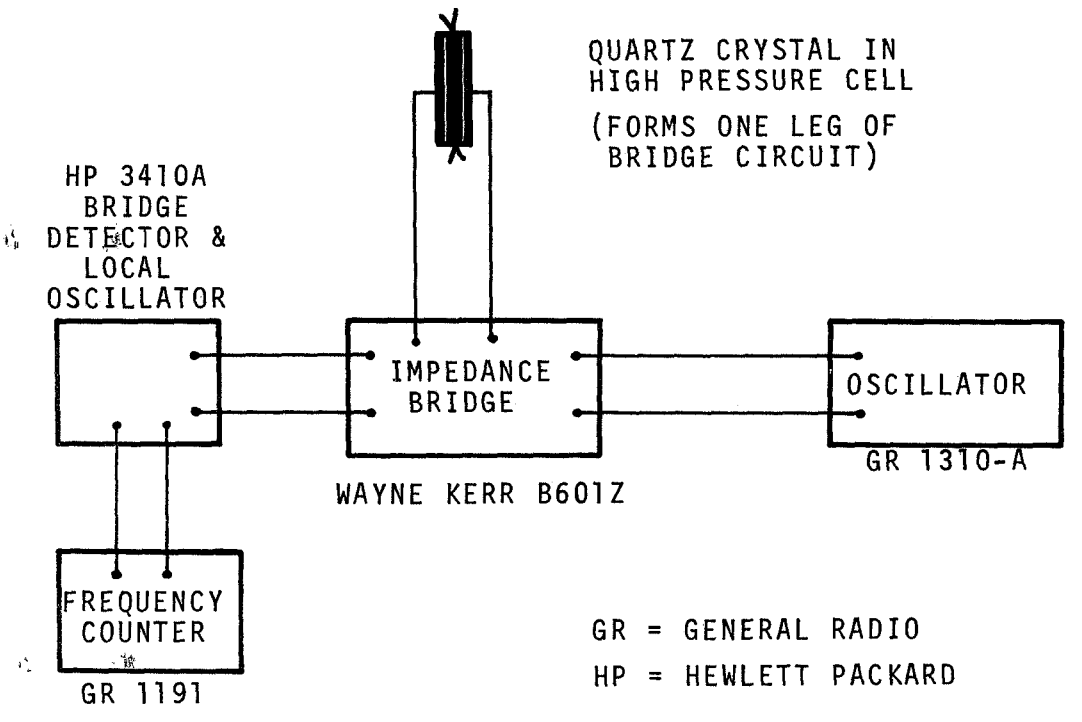

NOTE: ALL LEADS ARE SHIELDED.

Figure 3. Electronic Equipment Required for Measurements.

frequency measurements will be precise to ± 0.1 Hz. This precision is necessary because viscosity calculations depend on the difference between the resonant frequency in the test fluid and the inviscid fluid, or $f - f_o$. For more viscous fluids the difference between f and f_o is greater; in this case a gate time of one second was used and the resulting frequency measurements were precise to within ± one Hz.

The detector has a narrow band filter which is advantageous because it eliminated the effects of stray or undesired signals from the bridge balance. Incorporated in the detector is a local oscillator, which is driven at the same frequency as the impedance bridge. Since the local oscillator was used to drive the counter, correct frequency measurements were assured.

The quartz crystal is the sensor for viscosity measurements. Preparation of the crystal was the same as described by Rein (14) except that the ring of silver paint at the crystal midpoint was omitted and the electrodes were separated by tape during silver deposition. When the tape was removed following deposition, the electrodes remained effectively separated. This technique of electrode separation is superior to the earlier technique because it eliminated unnecessary crystal abrasion.

The quartz crystal must be securely mounted to insure reproducible results since the slightest slippage of the crystal can cause a significant change in the resonant frequency (as determined by calibration with an inviscid fluid) which in turn will introduce an appreciable error in the calculated viscosities.

Soldered electrical leads have been found to be unreliable mountings (15) because the leads often break off from the crystal. For this reason subsequent investigators have employed a spring-clamp mounting (1, 14). However, for this study a superior mounting was devised; it is shown in Figures 4 and 5. Its main advantage is that the crystal is supported at the crystal ends so that the electrical leads are not required to support the weight of the crystal. Further, reliable electrical contact to the crystal is attained by contacts in set screws which can

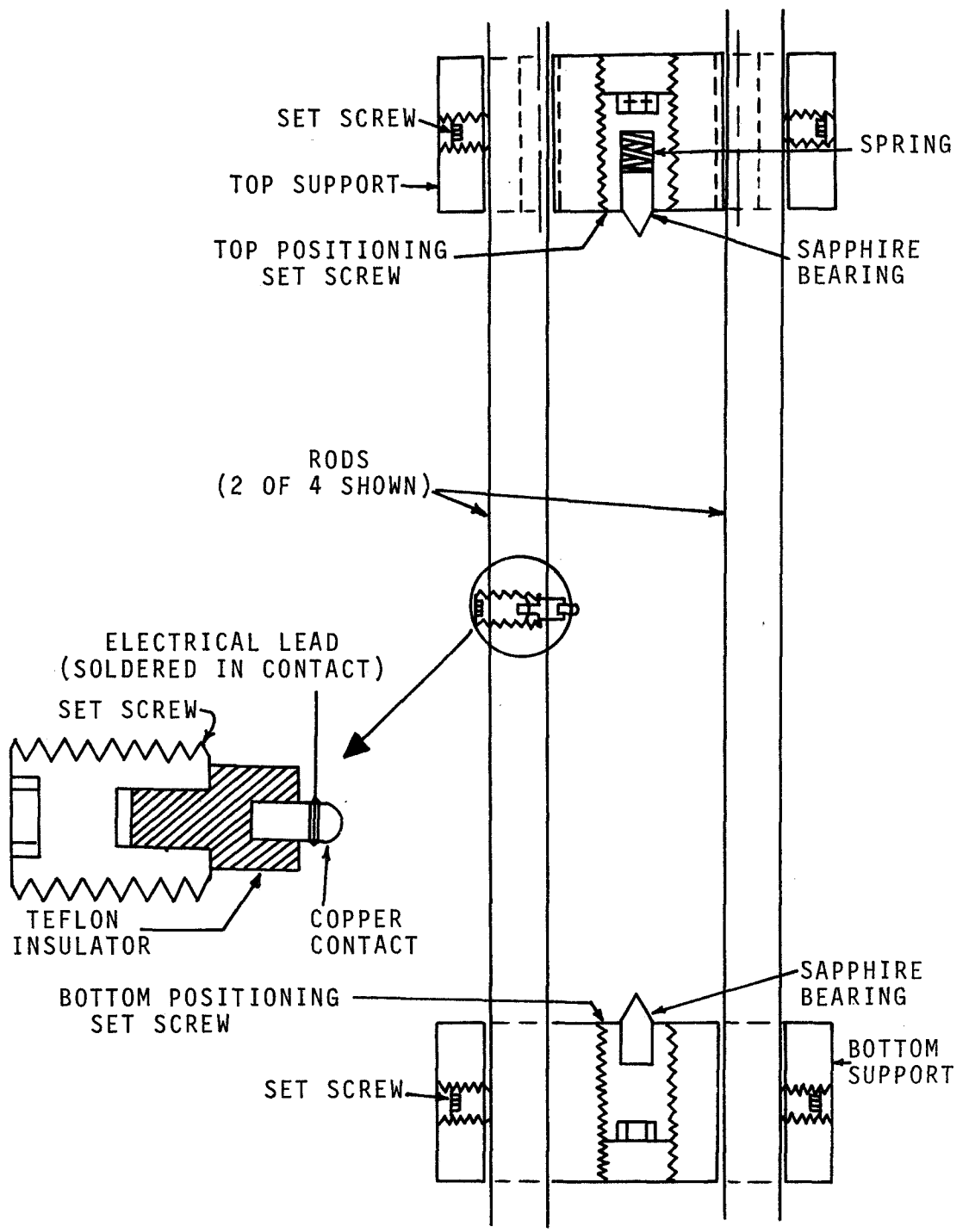

Figure 4. Details of an Improved Crystal Mounting.

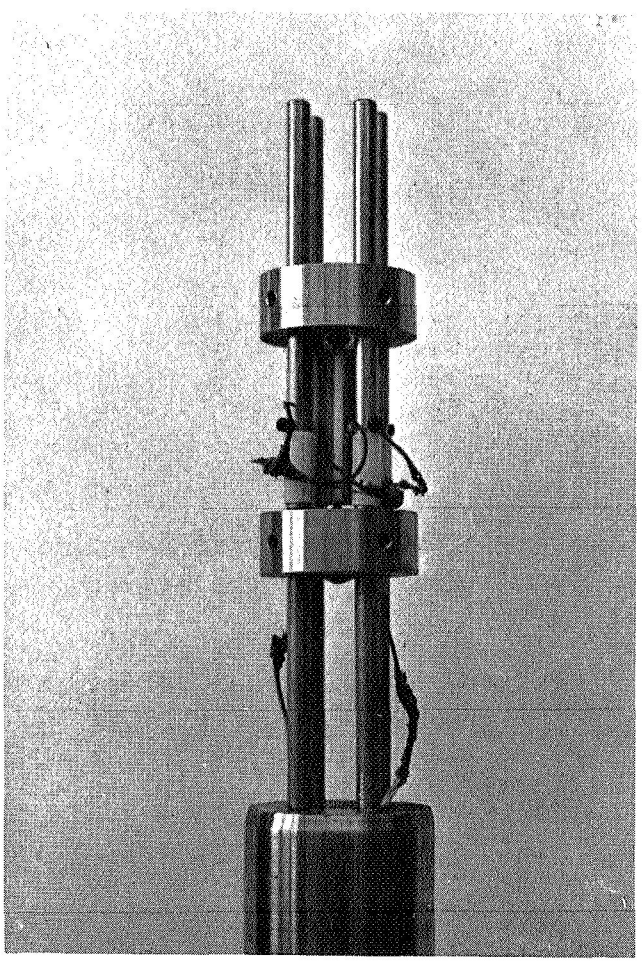

Figure 5. The 60 kHz Crystal in the Improved Mounting.

be advanced to maintain contact with the crystal as shown in Figure 4.

Viscosity Measurements

Prior to making viscosity measurements on the test fluids, a rather time-consuming calibration procedure was required. To facilitate this exposition and to demonstrate the methods for reducing the raw data, a brief review of the pertinent equations follows.

Pertinent equations: Viscosity measurements by the oscillating quartz crystal technique are interpreted in terms of a complex viscosity ($\eta^* = \eta_1 - i\eta_2$) or complex shear modulus ($G^* = G_1 + iG_2 = i\omega\eta^*$) which is related to the mechanical impedance, $Z_M = R_M + iX_M$, of the oscillating rod by

$$\eta_1 = G_2/\omega = 2X_M R_M/\omega\rho \qquad (1)$$

$$\eta_2 = G_1/\omega = (R_M^2 - X_M^2)/\omega\rho \qquad (2)$$

where ρ is the fluid density and $\omega = 2\pi f$ is the angular frequency of the rod. η_1 (or G_2) relates to viscous behavior, while G_1 (or η_2) relates to elastic behavior of the fluid.

X_M and R_M are related to the measured resonant frequency, f, in a given fluid and to the measured resistance at resonance, R_E, at the particular temperature and pressure, by

$$X_M = (f_o - f)/K_f \qquad (3)$$

and

$$R_M = (R_E - R_{Eo})/K_r \qquad (4)$$

where the subscript o refers to values obtained in an inviscid fluid. K_r and K_f are related to crystal properties and can be calculated (1, 15) or obtained from calibrations in Newtonian fluids of known viscosity and density (1, 4, 10, 11, 14, 15).

Manipulation of Equations 1, 3 and 4 shows that

$$R_E = R_{Eo} + K_r (\omega\rho\eta/2)^{1/2} \quad (5)$$

$$f = f_o - K_f (\omega\rho\eta/2)^{1/2} \quad (6)$$

for Newtonian fluids (for which $X_M = R_M$). Thus, it is apparent that K_r is the slope, and R_{Eo} the intercept, of the R_E versus $(\omega\rho\eta/2)^{1/2}$ curve. Likewise, K_f is minus the slope, and f_o the intercept, of the f versus $(\omega\rho\eta/2)^{1/2}$ curve. Therefore, for different Newtonian fluids with known viscosity and density, plots of $(\omega\rho\eta/2)^{1/2}$ versus resonant frequency and resistance give the desired calibration constants.

In addition, K_r and K_f are related to physical properties of the crystal by the following equations (1, 15).

$$K_f = (\pi\rho_c)^{-1}(r^{-1} + h^{-1}) \quad (7)$$

$$K_r = 4\pi L_c K_f \quad (8)$$

$$L_c = (2\pi\Delta f G_c)^{-1} \quad (9)$$

where r = the crystal radius
h = the length of the crystal
ρ_c = the crystal density
G_c = the conductance at resonance or the reciprocal of the resistance at resonance
Δf = the difference between the two frequencies at which the conductance is 1/2 the minimum value.

Calibrations based on Equations 5 and 6 are preferred to use of Equations 7, 8 and 9 because Equations 5 and 6 are more directly related to the actual measurements. K_r, K_f and R_{Eo} have been reported to be independent of pressure (1, 14). Also, a change in f_o with pressure has been reported (13). Therefore, calibrations were obtained at all temperatures and pressures at which lubricant viscosities were to be measured in order to

confirm the effect of pressure on f_o, to determine the effect of temperature on f_o, and to validate the invariance of K_r, K_f and R_{Eo} with pressure. Since the oscillating quartz crystal viscometer technique had not been used previously under the combined conditions of high temperature and high pressure, these calibrations served two additional purposes: to determine whether the simultaneous application of high temperature and high pressure had any effect on the pertinent parameters or on the stability of the crystal mounting. Although no effect on the pertinent parameters, per se, was detectable, some erratic behavior was encountered in attempts to make measurements at the highest temperature (482°F) which might be attributable to the delicacy of the crystal mounting.

Values of the viscosity and elastic modulus obtained at discrete frequencies and at various pressures and temperatures can be converted to equivalent values at a single temperature and pressure and over a range of frequencies by use of the concept of reduced variables (1, 8, 11). As applied to this investigation, the reduced variables concept states that increasing pressure, or decreasing temperature, has the same effect on viscosity or elastic modulus as increasing shear rate.

The reduced variables are defined by (1):

$$f_r = a_{TP} f \tag{10}$$

$$a_{TP} = (T_o/T)(\rho_o/\rho)(\eta_T/\eta_o)_P(\eta_P/\eta_o)_T \tag{11}$$

$$G_{1r} = G_1(T_o\rho_o/T\rho) \tag{12}$$

$$\eta_{1r} = \eta_1(\eta_o/\eta_T)_P(\eta_o/\eta_P)_T \tag{13}$$

where the subscripts T and P refer to the temperature and pressure of measurement and the subscript o refers to values at the common temperature and pressure to which all measurements are being reduced. The viscosities η_o, η_T and η_P are those measured in the limit of zero shear rate.

Calibrations: The fluids selected for calibration purposes were methylcyclohexane, n-pentane and di-(2-ethylhexyl) sebacate since their viscosities and densities over the range of pressures and temperature of interest were available.

The first step in the calibration procedure was to measure the resistance of the quartz crystal as a function of the frequency of the crystal when immersed in an inviscid fluid (either a vacuum or air at ambient conditions). Similar measurements were then made with the crystal immersed in a given fluid at a particular temperature and pressure. These measurements were repeated for each fluid at the other prescribed levels of temperature and pressure pertinent to this study. The data on resistance versus frequency for each fluid at each level of temperature and pressure were subjected to a least squares, quadratic (or cubic, where necessary) fit to derive an equation which was then differentiated to obtain the minimum point. The frequency at which the resistance was found to be a minimum was taken to be the resonant frequency at that particular temperature and pressure for the given fluid.

It should be understood that this same procedure had to be exercised for each test fluid as well as each calibration fluid. A typical plot is shown in Figure 6 for one of the test fluids, FN-3158, at 210°F and 20,200 psi, which is quite representative of the data obtained at all levels of temperature and pressure for both the calibration and test fluids. It should be noted that the abscissa in Figure 6 is given in terms of $(f - 19{,}900)$ rather than f. The only purpose in using this shift was to spread the data along the horizontal axis to facilitate visual examination.

After measurements on a fluid were completed, the cell and high pressure lines were flushed several times with petroleum ether to remove any remaining test fluid. The system was then put under vacuum for several hours. Next, the resonant frequency and resistance were checked in vacuum to determine if the cleaning had been effective. If the resonant frequency or resistance

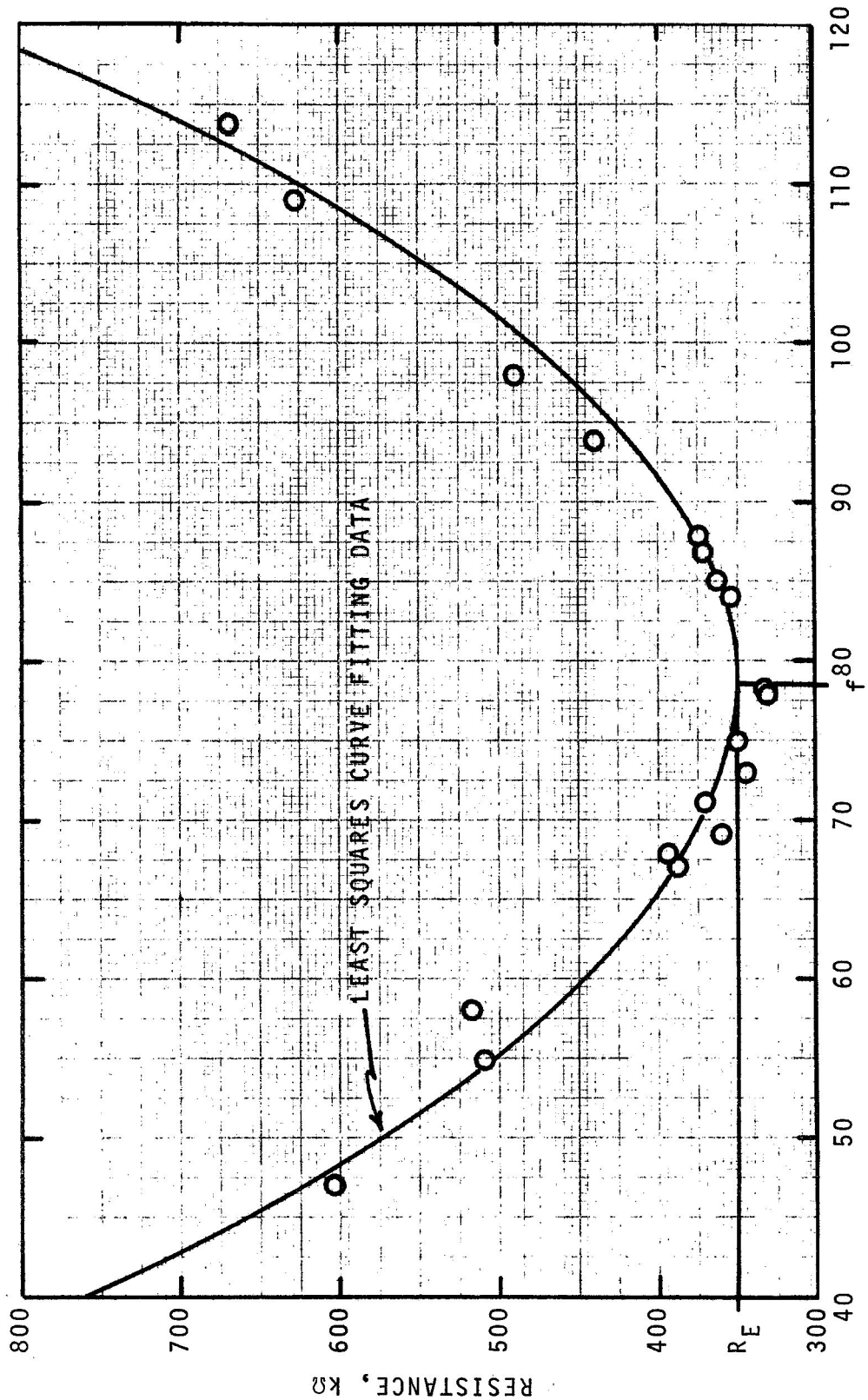

Figure 6. Typical Data for Determining Resonant Frequency. (Data for FN-3158 at 210°F and 20,200 psi.)

deviated significantly from the original values in a vacuum (or air), the cell was again flushed with petroleum ether and the test repeated. Measurements on the next fluid began only after it was obvious that the system was clean.

Having obtained the relationship between resonant frequency, f, and resistance, R_E, for the calibration fluids for which the viscosities and densities at various pressures and temperatures were known, it was possible to derive the calibration parameters, K_r, K_f, f_o and R_{Eo} as defined by Equations 1 through 4. It is evident from Equation 5 that a plot of R_E versus $(\omega\rho\eta/2)^{1/2}$ should yield a straight line having a slope of K_r and an intercept of R_{Eo} for each pressure and temperature level. Similarly, by Equation 6, a plot of f versus $(\omega\rho\eta/2)^{1/2}$ should yield a straight line having a slope of $-K_f$ and an intercept of f_o for each pressure and temperature level. The resulting values for these calibration parameters, K_r, K_f, f_o and R_{Eo} then reveal to what extent they are dependent on pressure and/or temperature.

The foregoing plotting technique was used for all calibration runs with the 20 kHz crystal. However, this method could be used to calibrate the 60 kHz crystal only at atmospheric pressure. At higher pressures, the inherent surface roughness of the 60 kHz crystal introduces intolerable uncertainties in the prediction of the calibration parameters (4). Measurements obtained with calibration fluids such as n-pentane or methylcyclohexane fall in the lower range of values for $(\omega\rho\eta/2)^{1/2}$ where surface roughness causes adverse effects. Since other fluids having known density and viscosity variations with pressure over the required range of high pressures are not available as calibration standards, the less preferred technique of using Equations 7 through 9 was employed to compute the calibration parameters at elevated pressures for the 60 kHz crystal.

Although methylcyclohexane and n-pentane were suitable for all calibration runs on the 20 kHz crystal, di-(2-ethylhexyl) sebacate could be used only over a limited range of pressures and temperatures as a calibration medium. As will be discussed

later, it demonstrates viscoelastic behavior at higher pressures and lower temperatures (below 300°F).

The required data on viscosity and density as functions of temperature and pressure for di-(2-ethylhexyl) sebacate were obtained from the ASME studies (2). Viscosity versus pressure data at 86 and 167°F from Bridgman (5) were interpolated to obtain viscosity-pressure information at 100°F for n-pentane and methylcyclohexane. These same data were also extrapolated to 210°F and 300°F to obtain the required viscosity-pressure information. Density-pressure information for n-pentane at 100 and 210°F was obtained by interpolation and extrapolation of data reported by Bridgman (6).

The remaining density information for use in calibrations had to be calculated because experimental data are not available. Density calculations were based on a corresponding states scheme (12).

Figure 7 is representative of calibrations to obtain K_r and R_{Eo} for the 20 kHz viscometer. Since it includes data for all temperature measurements, the good correlations suggest the absence of a temperature effect of K_r, which confirms conclusions reached by others (1). R_{Eo} was found to be independent of pressure and temperature in accordance with other investigations (1). However, in contrast to the results reported by others (1, 14), K_r was found to depend on pressure, as indicated in Figure 7. A close inspection of the data given by Appledoorn, et al. (1) indicates a small change in K_r with pressure. Since the magnitude of this variation would have a neglible effect on their results, it might have been overlooked. Uncertainties in data may have masked any changes in K_r with pressure in Rein's earlier work (14).

As explained before, the calibration parameters for the 60 kHz crystal at elevated pressures had to be calculated from Equations 7 through 9. The calculated values for K_r for the 60 kHz crystal likewise showed a variation with pressure.

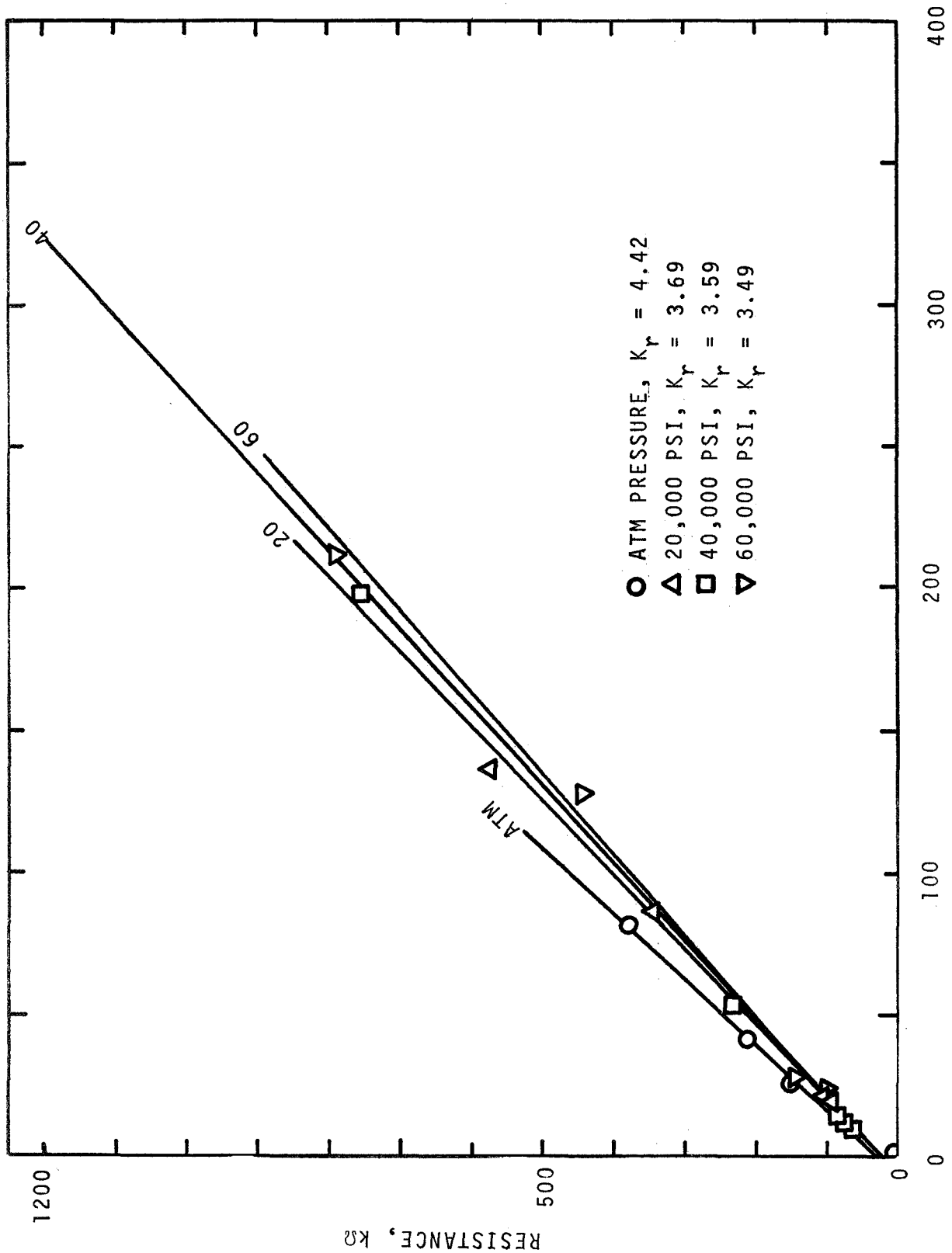

Figure 7. Typical Resistance Calibration Data. (Data from Run 20 kHz-II.)

The dependency of K_r on pressure for both crystals is summarized in Figure 8.

Figure 9 is representative of calibrations to obtain K_f and f_o for the 20 kHz crystal. As indicated by the random variation in K_f with pressure, it was concluded that K_f was independent of pressure which is consistent with previous observations (1, 14). K_f was also found to be independent of temperature, again in agreement with conclusions by others (1). The change in f_o with pressure at 100°F as found in this study is in accord--at least within experimental error--with others (13). Since f_o also varies with temperature, it had to be determined at every temperature and pressure for which viscosity measurements were to be made on the four test fluids.

Table I summarizes the principal outputs from the calibration runs.

Density Determinations

It is apparent from Equations 1 and 2 that the density of the fluid must be known in order to compute the viscosities. Since density data at the different levels of temperature and pressure were not available for the four test fluids, they had to be measured in the course of this contract. The procedure consisted of introducing the test fluid into the pressure cell by means of the intensifier (refer to Figures 1 and 2). The cell is maintained at the desired temperature level. The mass of test fluid introduced into the cell to attain a prescribed pressure was determined from the intensifier piston travel which, in turn, was indicated by the amount of pressurizing oil displaced into the sight glass. The experimental procedure and data reduction are elucidated in the following derivation of the pertinent equations.

The mass of fluid introduced into the pressure cell, dm_{cell}, is equal to the mass of fluid displaced by the intensifier piston, $-dm_{inten}$. Thus,

$$dm_{cell} = -dm_{inten} = \rho_{inten} A d\ell \qquad (14)$$

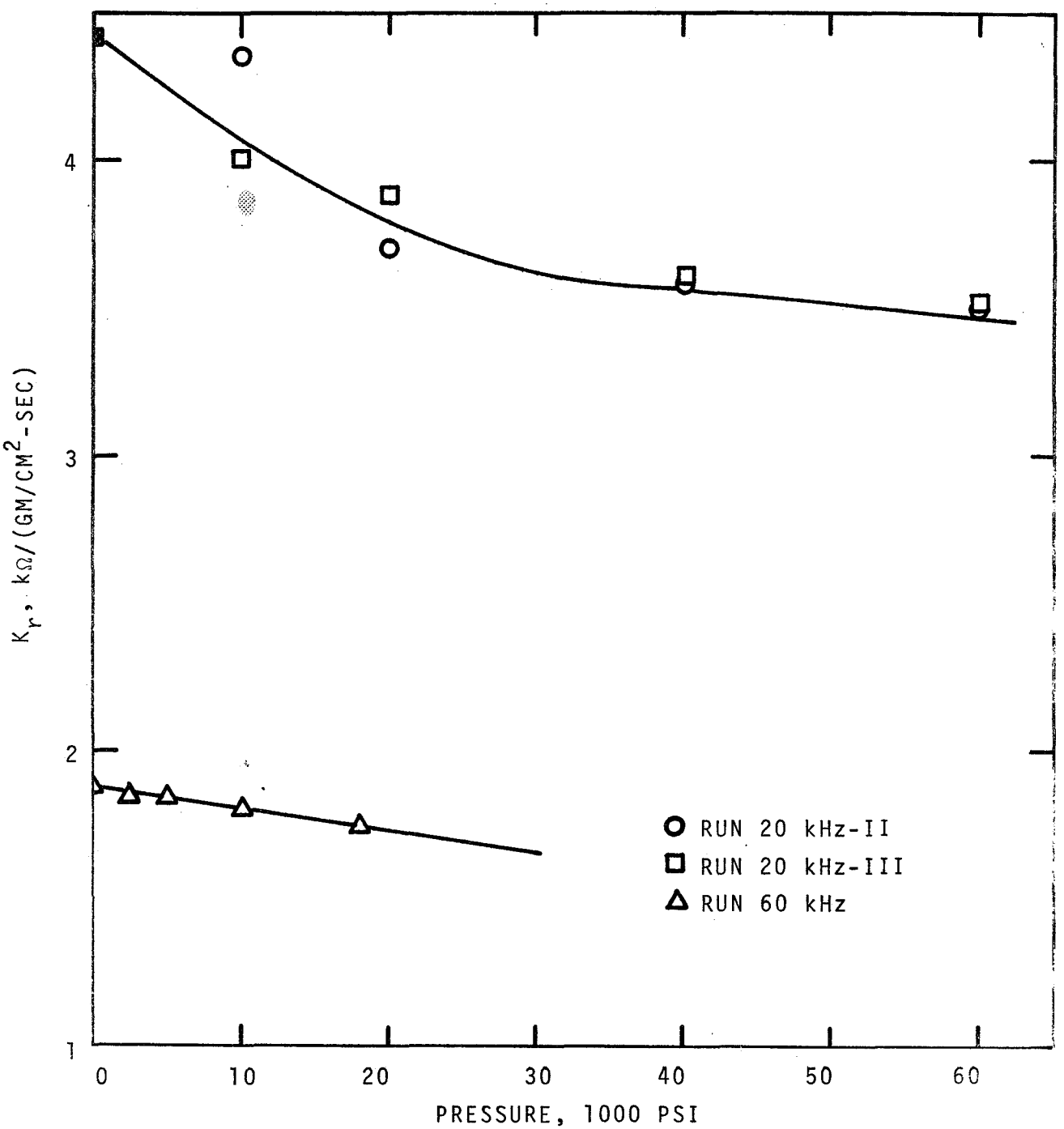

Figure 8. The Effect of Pressure on the Calibration Parameter, K_r.

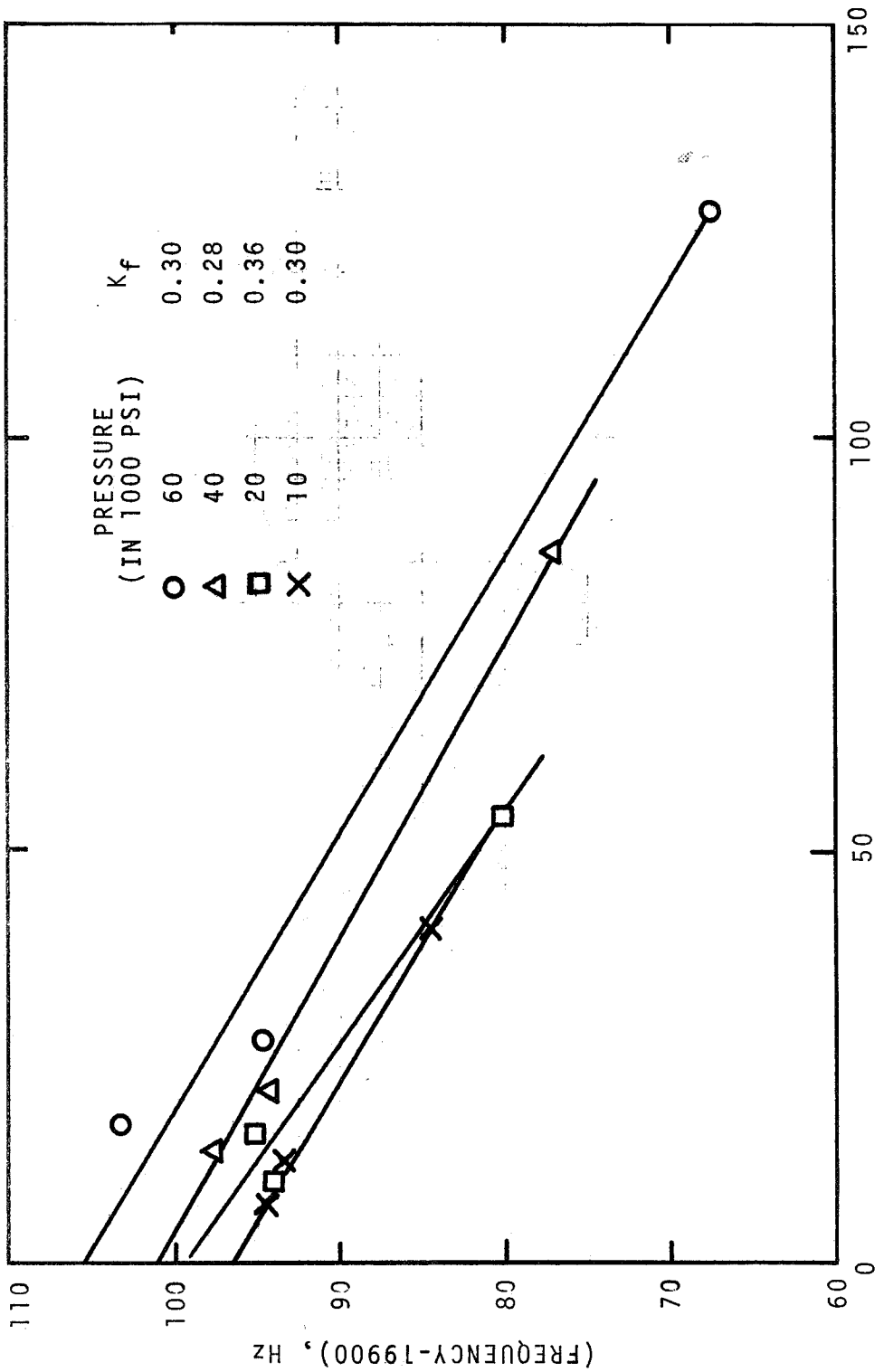

Figure 9. Typical Frequency Calibration Data. (Data from Run 20 kHz-III at 300°F.)

TABLE I

CALIBRATION PARAMETERS FOR EACH DATA RUN

Crystal*	Parameter	Value	Comments
20 kHz-II	K_f	0.32	Independent of temperature and pressure
	K_r		Independent of temperature, dependent on pressure as shown in Figure 8
	f_o		Empirically determined for each temperature and pressure of measurement
	R_{Eo}	31.6 kΩ	Independent of temperature and pressure
20 kHz-III	K_f	0.30	Independent of temperature and pressure
	K_r		Independent of temperature, dependent on pressure as shown in Figure 8
	f_o		Empirically determined for each temperature and pressure of measurement
	R_{Eo}	30.4 kΩ	Independent of temperature and pressure
60kHz**	K_f	0.32	Independent of pressure
	K_r		Dependent on pressure as shown in Figure 8
	f_o		Determined from correlation in Reference 13
	R_{Eo}	0Ω	Independent of pressure

*20 kHz-II and -III designate re-mounting of the crystal. Calibrations for runs -0 and -I were not obtained because of high pressure equipment failures during these runs.

**The temperature was constant during all of these runs so no variation in parameters with temperature could be observed.

where A is the cross sectional area of the high pressure piston, ρ_{inten} is the density of the fluid in the intensifier at the existing pressure and temperature of the intensifier, and $d\ell$ is the piston movement during pressurization.

The total mass in the cell at any pressure is the mass that was present at atmospheric pressure, m_o, and the amount added during pressurization. Thus,

$$m_{cell} = m_o + \int dm_{cell} = m_o + \int \rho_{inten} A d\ell \qquad (15)$$

Division of Equation 15 by the volume of the cell, V, a constant, gives

$$\rho = \rho_{cell} = \rho_o + (A/V) \int \rho_{inten} A d\ell$$

$$= \rho_o + (A/V) \int \rho_{inten} (\partial\ell/\partial P)_T \, dP \qquad (16)$$

where ρ = the fluid density at a given temperature and elevated pressure

ρ_o = the fluid density at the given temperature and atmospheric pressure

A = the cross sectional area of the high pressure intensifier piston

V = the volume of the high pressure cell

$(\partial\ell/\partial P)_T$ = the slope of the piston displacement-pressure curve. The restriction of constant temperature was satisfied by carrying out the compression slowly.

The cell volume, V, in Equation 16 can be approximated closely by

V = Total internal volume of cell - Crystal volume - Volume of viscometer support

From the measured dimensions of these quantities, the cell volume, V, was calculated to be 60.9 in^3.

The high pressure piston had a diameter of 0.625 inches (thus, a cross sectional area of 0.307 in^2) during all measurements, except for the runs with Humble FN-3158 fluid. In this latter case an oversize piston having a diameter of 0.660 inches (cross sectional area of 0.342 in^2) was used.

In addition to the values of V and A obtained above, it is necessary to know ρ_{inten} as a function of pressure at the intensifier temperature. Based on the material balance of Equation 14, and restricting it to the case of equal cell and intensifier temperatures, the following finite difference equation was used to determine ρ_{inten} as a function of pressure:

$$\rho_{n+1} - \rho_n = [1 + (A/2V)\Delta\ell_T]/[1 - (A/2V)\Delta\ell_T] \qquad (17)$$

$\Delta\ell$ represents the piston displacement during a given pressure change and the subscript T indicates that the intensifier and cell must be at the same temperature. Densities of the test fluids were measured at temperatures above room temperature and the intensifier was always at room temperature. Thus no measurements were made in which the cell and intensifier were actually at the same temperature. Therefore, $\Delta\ell_T$, at given constant pressures, was obtained by extrapolation of the measured values of $\Delta\ell$ at the various temperatures to the intensifier temperature.

The foregoing technique for measuring densities was validated by measuring the densities of one of the calibration fluids, di-(2-ethylhexyl) sebacate, for which density data were available in the literature. Table II compares these values and demonstrates an agreement within ± one percent.

TABLE II

A COMPARISON OF DENSITY VALUES FOR
DI-(2-ETHYLHEXYL) SEBACATE

Temp. (°F)	Press. (1000 psi)	ρ (This Project) (gm/cc)	ρ (Reference 2) (gm/cc)
100	10	0.939	0.941
	20	0.968	0.965
	40	1.008	1.007
	60	1.034	1.037
	80	1.057	1.064
210	10	0.903	0.906
	20	0.938	0.934
	40	0.985	0.982
	60	1.014	1.013
	80	1.037	1.064
	100	1.067	1.064
300*	10	0.870	0.879
	20	0.908	0.913
	40	0.960	0.963
	60	0.989	0.997
482**	10	0.813	0.832
	20	0.866	0.874
	40	0.935	0.928
	60	0.968	0.965
	80	0.986	0.996
	100	1.013	1.023
	115	1.054	1.039

*Density values for Reference 2 were obtained by interpolation of known ρ(T) data at each pressure.

**Density values for Reference 2 were obtained by extrapolation of known ρ(T) to 482°F at each pressure.

RESULTS

Having determined the calibration parameters, f_o, K_f, K_r and R_{Eo}, for the viscometer, measurements of frequency and resistance of the crystal in the four test fluids as well as the density of the fluids are required at the various levels of temperature and pressure in order to calculate the viscosities from Equations 1 and 2. The experimental procedures are identical to the calibration exercises described previously. This section presents the results of the density and viscosity determinations.

In addition (although not part of the contractural requirements) the observations of viscoelastic behavior are discussed briefly as relevant information. Indications of viscoelastic behavior in Mobil XRM-109 and Humble FN-3158 plus 10 volume percent Kendall 0839 were found at 100°F, but sufficient data were not obtained to be conclusive. However, to illustrate the analysis for viscoelasticity, the results obtained with one of the calibration fluids, di-(2-ethylhexyl) sebacate, are presented.

Density

The densities of the four test fluids as functions of pressure at different temperature levels are summarized in Figures 10, 11 and 12. The densities at atmospheric pressure for various temperatures were obtained by interpolation and extrapolation of data supplied by NASA (9) as shown in Figure 13. Tabulated density data are given in Appendix A.

As could be expected, the density-pressure curves for Humble FN-3158 and the mixture FN-3158 plus 10 volume percent Kendall 0839 were found to be essentially identical. The density of each of these components is similar at atmospheric pressure, and apparently the presence of 10 volume percent of Kendall 0839 does not introduce any deviations from additive volume behavior.

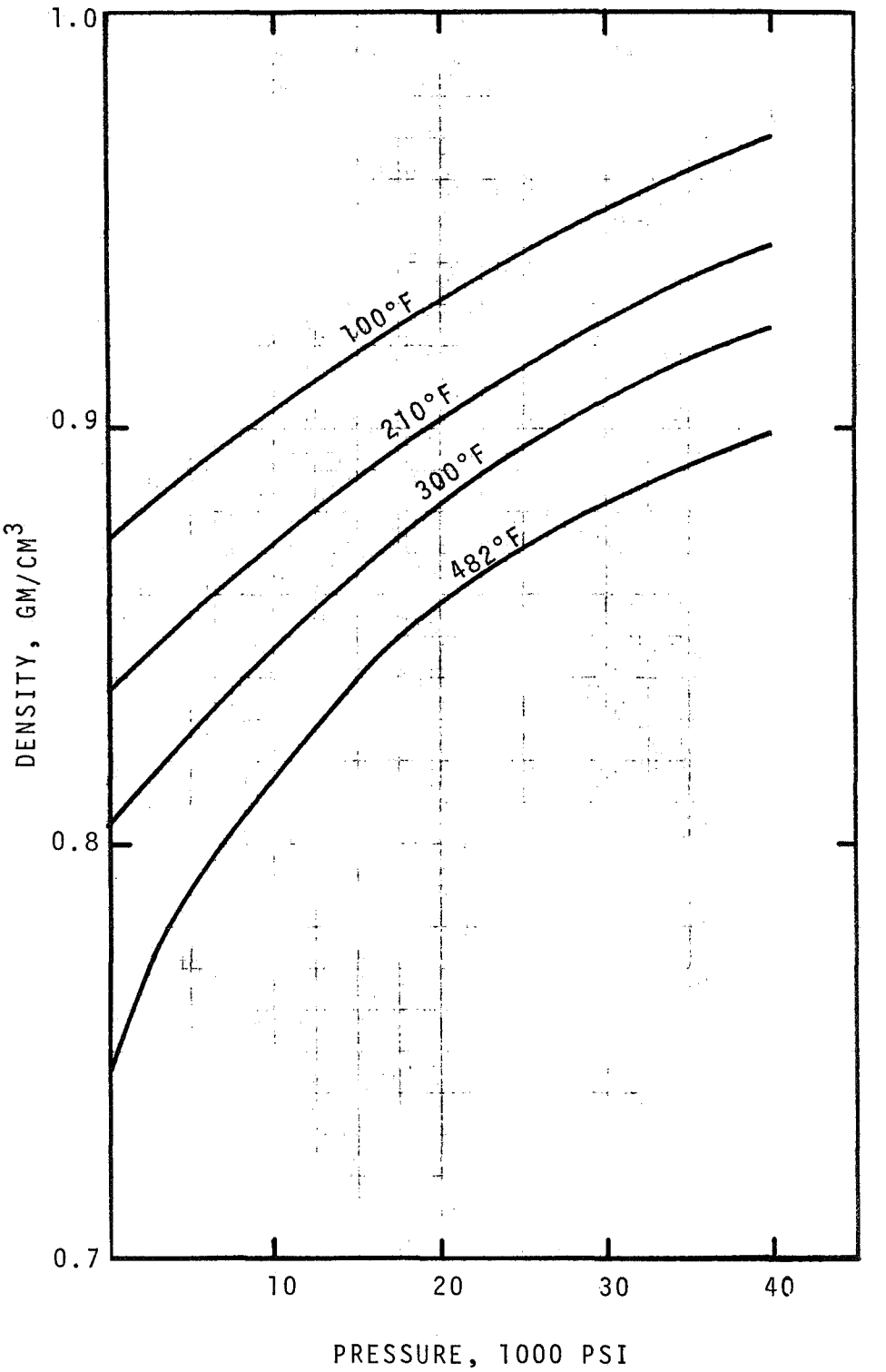

Figure 10. The Effects of Pressure and Temperature on the Densities of Humble FN-3158 and Humble FN-3158 + 10 vol % Kendal 0839.

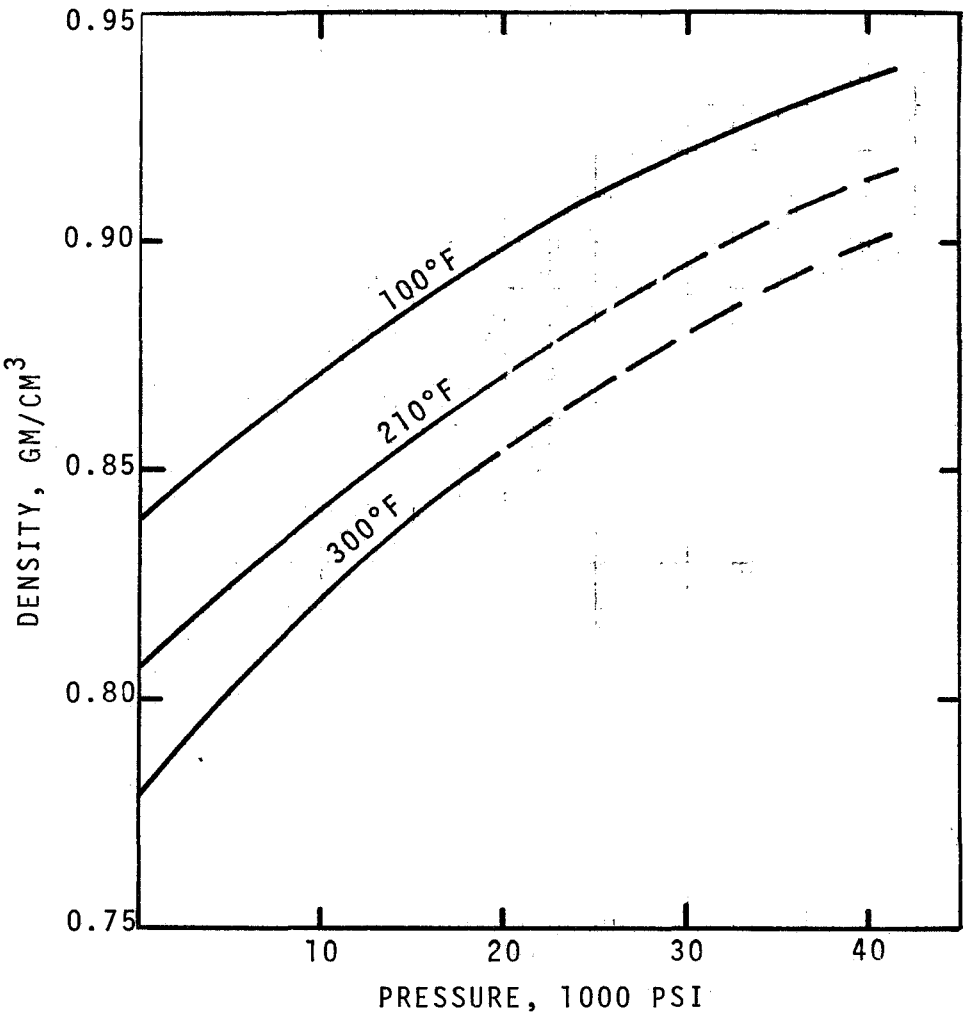

Figure 11. The Effects of Pressure and Temperature on the Density of Mobil XRM-109.

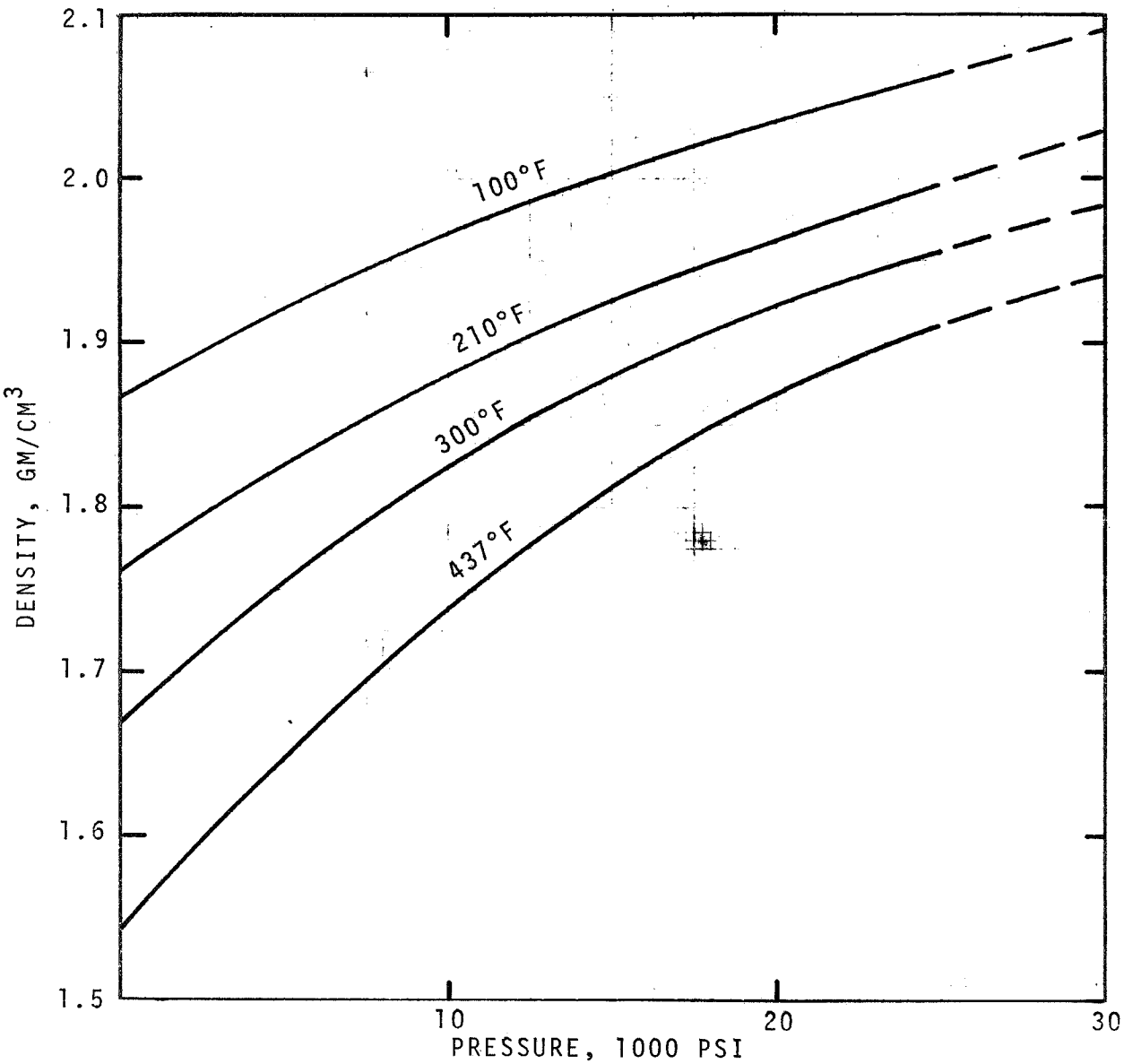

Figure 12. The Effects of Pressure and Temperature on the Density of DuPont Krytox 143-AB.

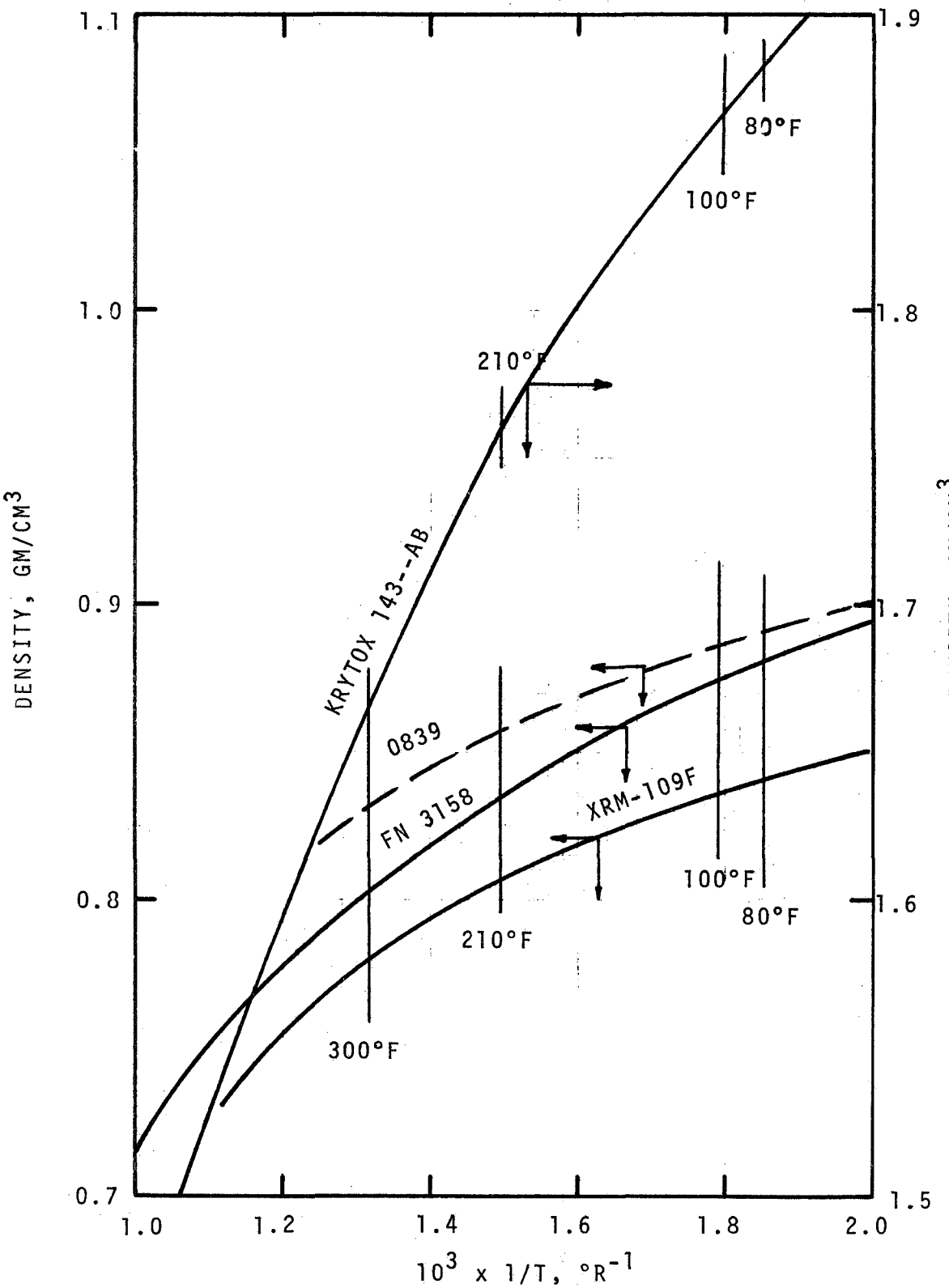

Figure 13. Density of Test Fluids at Atmospheric Pressure. (Data from Reference 9.)

Viscosity

Figures 14, 15, 16 and 17 summarize the results of the viscosity measurements for the test fluids as functions of pressure at different temperatures. Tabulated data are given in Appendix B. The viscosity data are estimated to be accurate with ± 15 percent. It will be noted in Figure 17 that viscosity data for DuPont Krytox 143-AB are given only at 100°F. Although data were taken at higher temperatures, they were not considered sufficiently reliable to report. Upon completion of the higher temperature runs, the pressure cell was opened. Examination of the crystal mounting revealed that it was not true. Time was not available to repeat these runs at the higher temperatures, particularly since the GR 1310-A oscillator was in need of maintenance which required a down-time of several weeks.

For the sake of comparison, the viscosities of the four test fluids at atmospheric pressure at temperatures of 74.3°, 112°, 130° and 190°F were determined by means of a Canon-Fenske capillary viscometer. These data are summarized in Figure 18. No attempt was made to extrapolate these data beyond 210°F because of the uncertainties involved. The capillary values are shown on the zero gauge pressure ordinate for the 100° and 210°F isotherms in Figure 14 through 17. The discrepancies between the two methods of measurement are within the estimated accuracy of ± 15 percent for the oscillating quartz crystal viscometer.

Viscoelastic Behavior

Although the work statement for this contract did not include determination of the viscoelastic effect, the fact that two of the test fluids, Mobil XRM-109 and Humble FN-3158 plus 10 volume percent Kendall 0839, gave indications of departure from Newtonian behavior merits mention.

The components of the complex viscosity of a fluid are given by

$$\eta^* = \eta_1 - i\eta_2 \qquad (18)$$

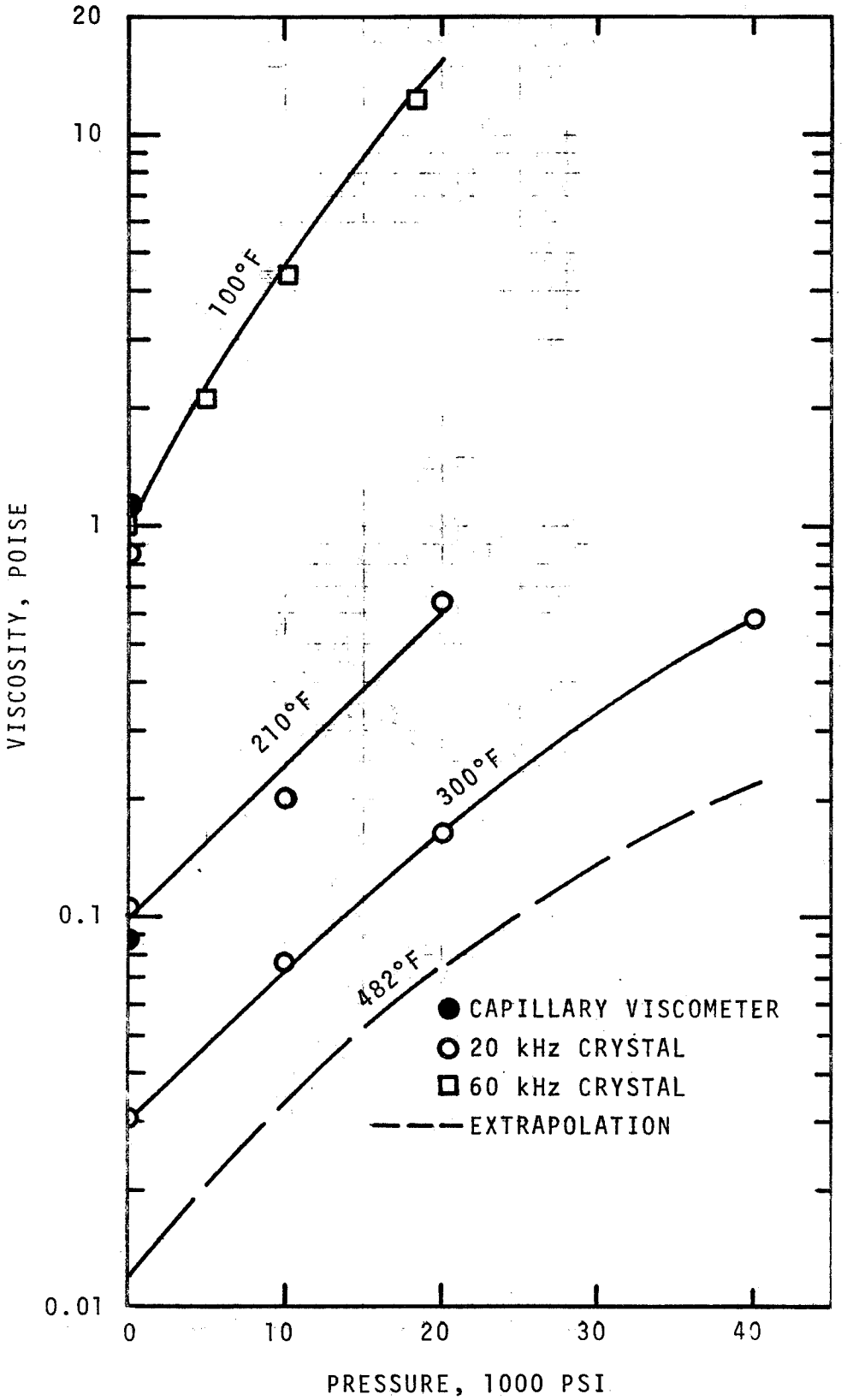

Figure 14. The Effects of Pressure and Temperature on the Viscosity of the Mixture of Humble FN-3158 + 10 vol % Kendall 0839.

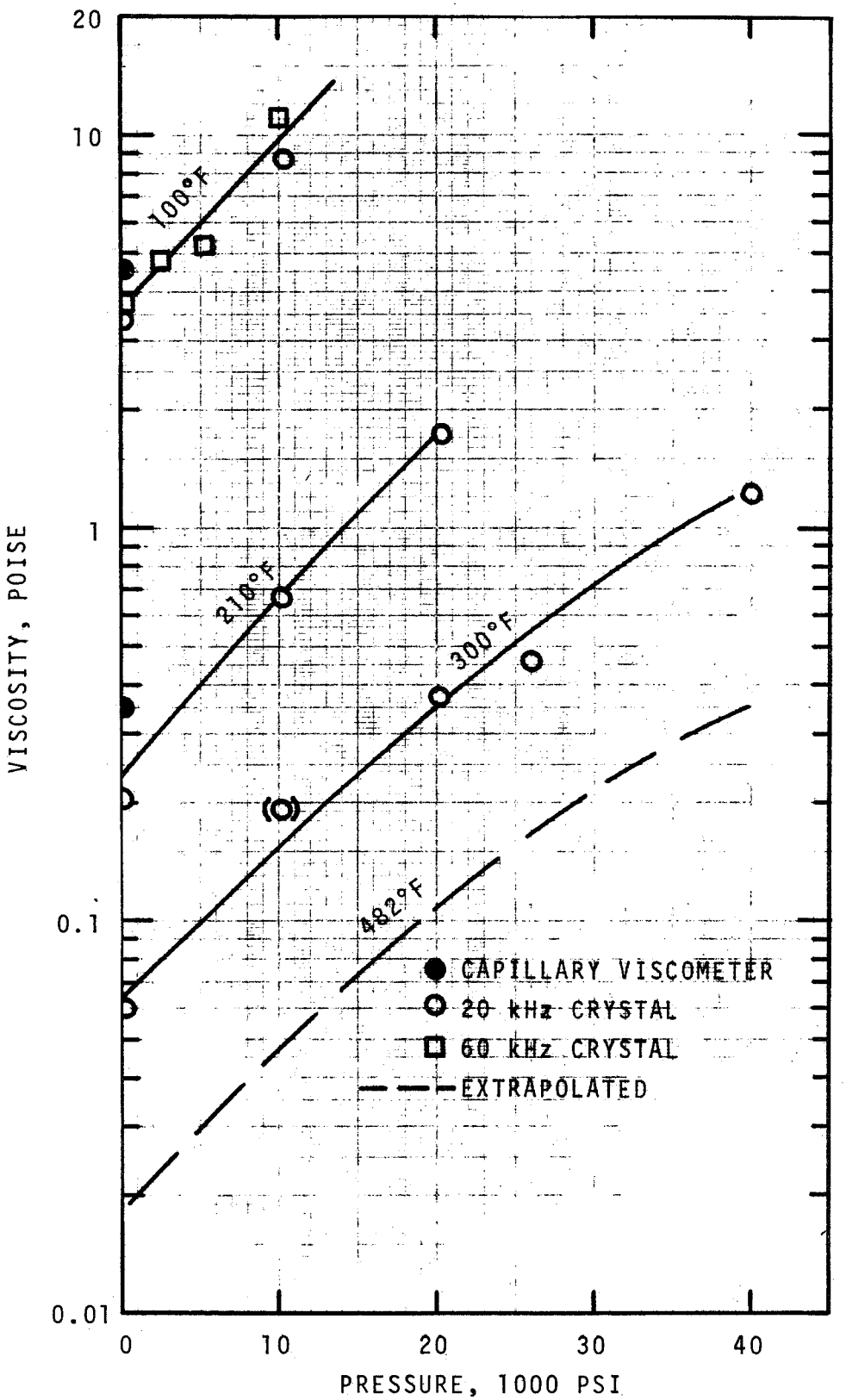

Figure 15. The Effects of Pressure and Temperature on the Viscosity of Mobil XRM-109.

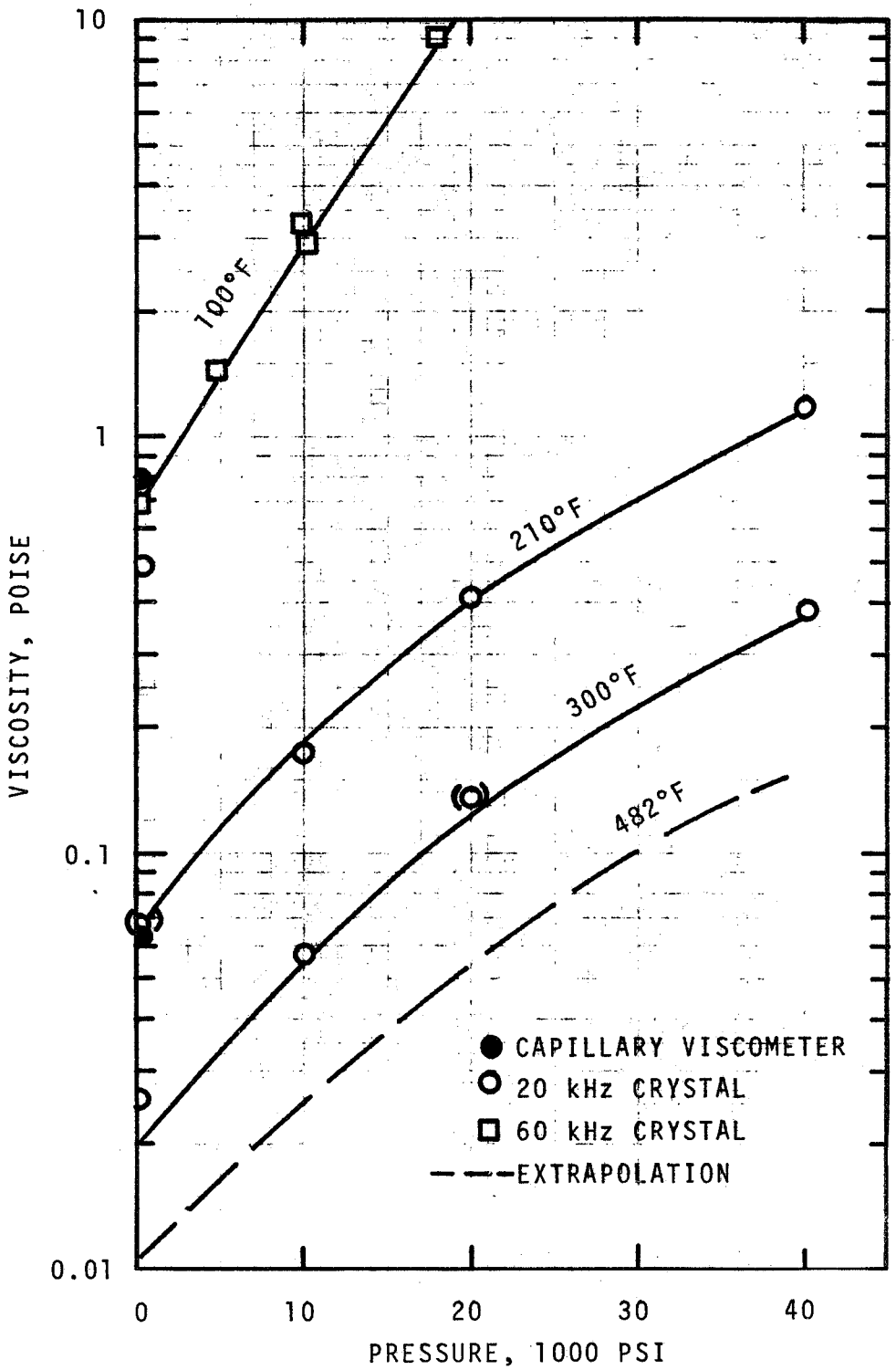

Figure 16. The Effects of Pressure and Temperature on the Viscosity of Humble FN-3158.

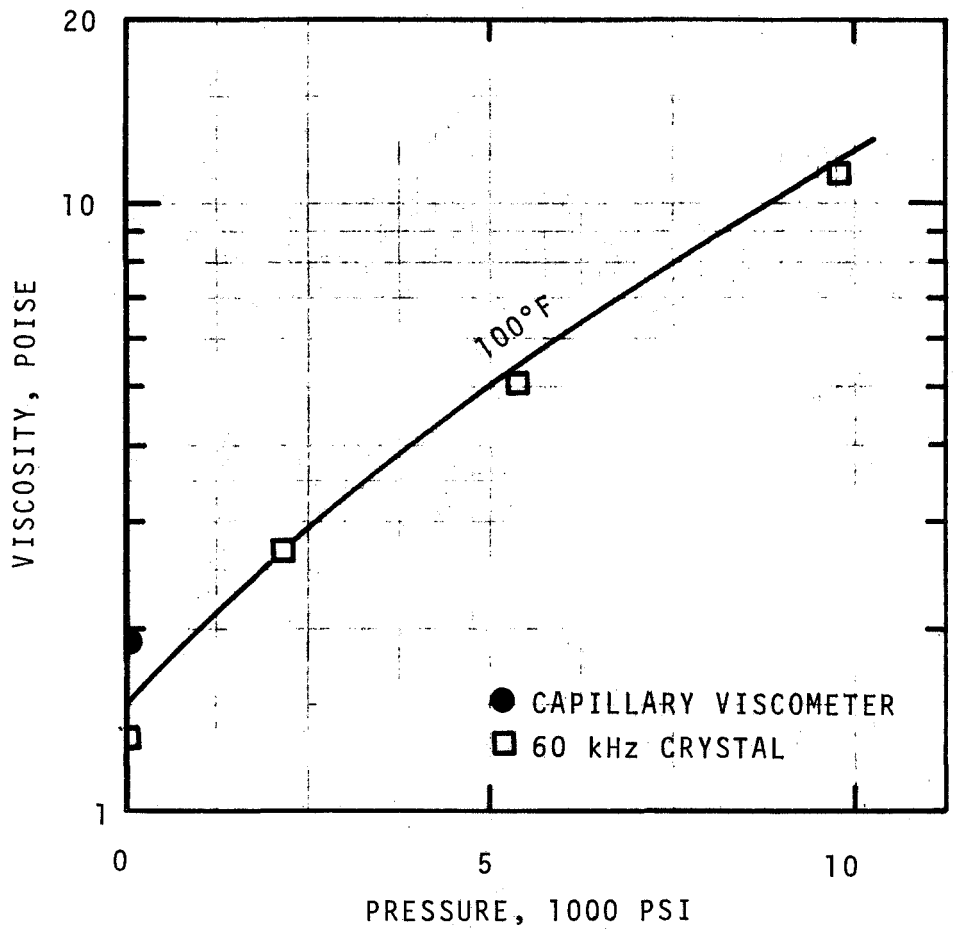

Figure 17. The Effect of Pressure on the Viscosity of Dupont Krytox 143-AB at 100°F.

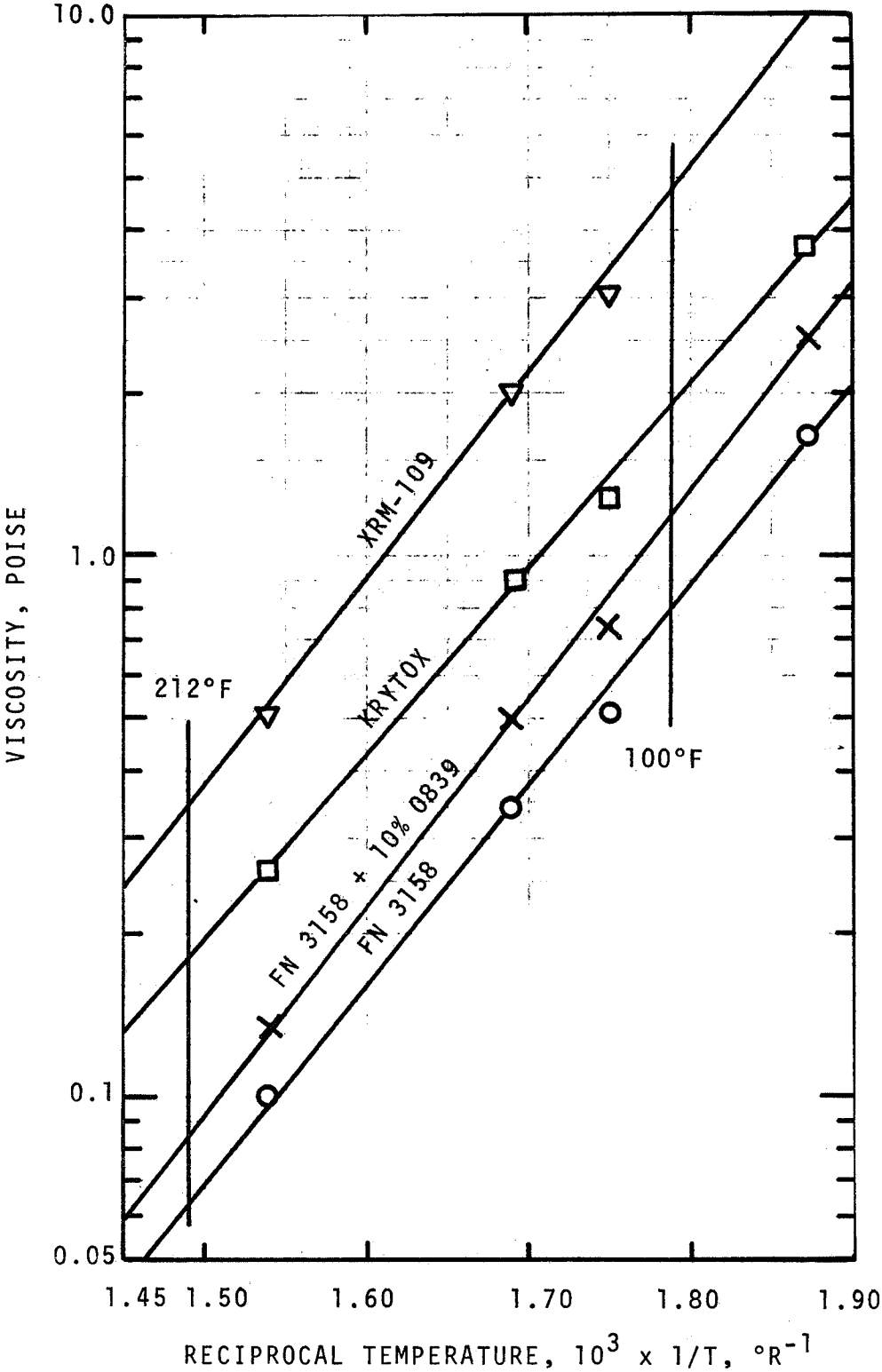

Figure 18. Viscosity as Determined from Capillary Viscometer at Atmospheric Pressure.

and the components of the complex shear modulus by

$$G^* = G_1 + iG_2 = i\omega\eta^* \tag{19}$$

Both are related to the mechanical reactance, X_M, and resistance, R_M, of the oscillating crystal by

$$\eta_1 = G_2/\omega = 2X_M R_M/\omega\rho \tag{1}$$

$$\eta_2 = G_1/\omega = (R_M^2 - X_M^2)/\omega\rho \tag{2}$$

where ρ is the fluid density and $\omega = 2\pi f$ is the angular frequency of the crystal, which is assumed to be equal to the shear rate. The mechanical impedance of the crystal, Z_M, is given by $R_M + iX_M$ where

$$R_M = (R_E - R_{Eo})/K_r \tag{4}$$

$$X_M = (f_o - f)/K_f \tag{3}$$

For a Newtonian fluid, $\eta^* = \eta_1$, since $\eta_2 = 0$ in Equation 18, which requires that $R_M = X_M$ according to Equation 2. However, if η_2 is non-zero, then $R_M \neq X_M$ and viscoelastic behavior is indicated.

A characteristic of the oscillating quartz viscometer is that the difference $(R_E - R_{Eo})$ in Equation 4 is much larger than the difference $(f_o - f)$ in Equation 3. For this reason, errors in measurements of resistance are less serious than errors in measurements of frequency for computing values of R_M and X_M, respectively. As the temperature of measurement increases and simultaneously the viscosity decreases, f approaches f_o much faster than R_E approaches R_{Eo}. Consequently, a loss in significant figures for the difference $(f_o - f)$ results. Because of this uncertainty, whenever the calculated values of R_M differed significantly from X_M for measurements at a particular temperature and pressure, whereas measurements on this fluid consistently

resulted in R_M being equal to X_M at other pressures and temperatures (for which a difference in R_M and X_M would have been more plausible) the calculation of viscosity, η_1, was based entirely on the more reliable resistance measurements. In this case Equation 1 becomes

$$\eta_1 = G_2/\omega = 2R_M^2/\omega\rho \quad (\text{for } \eta_2 = 0) \tag{20}$$

The viscosities which were calculated solely from Equation 20 are indicated by enclosing the data points in parentheses for the 300°F isotherm for Mobil XRM-109 in Figure 15 and the 210°F and 300°F isotherms for Humble FN-3158. Aside from these exceptions, both frequency and resistance measurements were used to compute the viscosities by means of Equations 1 and 2.

For all fluids at 100°F the difference $(f_o - f)$ retained sufficient significant figures so that reliance could be placed on the frequency, as well as the resistance, measurements. In other words, at 100°F equal confidence could be given to the values of η_1 and η_2 as computed from Equations 1 and 2. The components of complex viscosity, $\eta_1 - i\eta_2$, and the complex shear modulus, $G_1 + iG_2$, are summarized in Table III for Humble FN-3158 plus 10 volume percent Kendall 0839 and for Mobil XRM-109. For the other two fluids, Humble FN-3158 and DuPont Krytox 143-AB, η_2 was found to be zero. The shear rates in the fluid were obtained by making the usual assumption that they are equal to the angular frequency of the crystal, ω, which is defined as $\omega = 2\pi f$.

By resorting to the use of the concept of reduced variables, as defined by Equations 10 through 13, the onset of viscoelastic behavior is predicted at 100°F and atmospheric pressure for the following reduced angular frequencies (or shear rates):

TABLE III

VISCOELASTIC BEHAVIOR OF TEST FLUIDS AT 100°F

Fluid	Crystal kHz	Shear Rate sec^{-1}	Pressure psi	η_1 poise	η_2 poise	G_1 $dynes/cm^2$	G_2 $dynes/cm^2$
Humble FN-3158 plus 10 volume percent Kendall 0839	60	3.77×10^5	18,400	12.4	1.94	7.5×10^5	4.09×10^6
Mobil XRM-109	20	1.26×10^5	10,300	8.74	2.26	2.8×10^5	1.10×10^6
Mobil XRM-109	60	3.77×10^5	9,640	11.1	1.22	4.7×10^5	4.18×10^6

Fluid	Reduced Angular Frequencies
Humble FN-3158 plus 10 volume percent Kendall 0839	4.7×10^6 radians/sec
Mobil XRM-109	5.9×10^5 radians/sec

The frequencies listed above are at best approximate because viscosities at zero shear rate as a function of pressure and temperature, which are required to compute the reduced variables, were not available. Also, until more experimental data are obtained over a wider range of conditions, the conclusion of viscoelastic behavior for these two fluids at 100°F should be regarded as tentative.

The difficulty with the present design of the high pressure equipment is that it was not possible to make measurements above 40,000 psi because of the excessive viscosity of these fluids. Furthermore, at higher pressures, a deterioration of sensitivity in measurement was encountered. The principal advantage of going to higher pressures is that it would permit simulation of higher shear rates at atmospheric pressure by means of the concept of reduced variables. Further alleviation of the present limitations may be forthcoming with the 100 kHz crystal, which is now being prepared for preliminary testing in the viscometer. An alternative may be the use of another quartz crystal technique reported by Barlow and Lamb (8), for which shear rates of at least two orders of magnitude higher than the present oscillating quartz crystal can be simulated.

During the calibrations of the viscometer with di-(2-ethylhexyl) sebacate, it was observed that the measured frequency was significantly higher than would be expected for a Newtonian fluid for given values of $(\omega\rho\eta/2)^{1/2}$ at the higher pressures. The anomalous behavior was consistently observed for both crystals and for the several remountings of the 20 kHz crystal that were required during the course of the experimental work; these observations confirmed the existance of viscoelastic

behavior. The temperatures and pressures at which these deviations from Newtonian behavior were observed are summarized in Table IV.

TABLE IV

CONDITIONS FOR VISCOELASTIC BEHAVIOR OF DI-(2-ETHYLHEXYL) SEBACATE

Crystal	Temperature (°F)	Pressure (1000 psi)
60 kHz	100	10 and 18
20 kHz	100	10, 20, 40 and 60
20 kHz	210	20, 40 and 60

The concept of reduced variables was again employed to convert these observations with the two crystals at various temperatures and pressures to a common basis of 100°F and atmospheric pressure. Figure 19 shows the reduced elastic (storage) modulus, G_{lr}, as a function of reduced frequency. The results of previously reported observations on the viscoelastic behavior of di-(2-ethylhexyl) sebacate at much higher frequencies (8) are also shown. A least squares fit of the data from both of these investigations is given by the equation

$$G_{lr} = 0.189\ f_r^{0.977} \qquad (21)$$

with a correlation coefficient of 0.992. (Note that the data points taken from Reference 8 and shown on Figure 19 were read from a smoothed curve of R_M and X_M versus reduced frequency; thus they exhibit less scatter than the raw data from the present investigation.) Even though there is no overlap of the data between the two investigations, the high correlation coefficient indicates that both sets of results are in basic agreement.

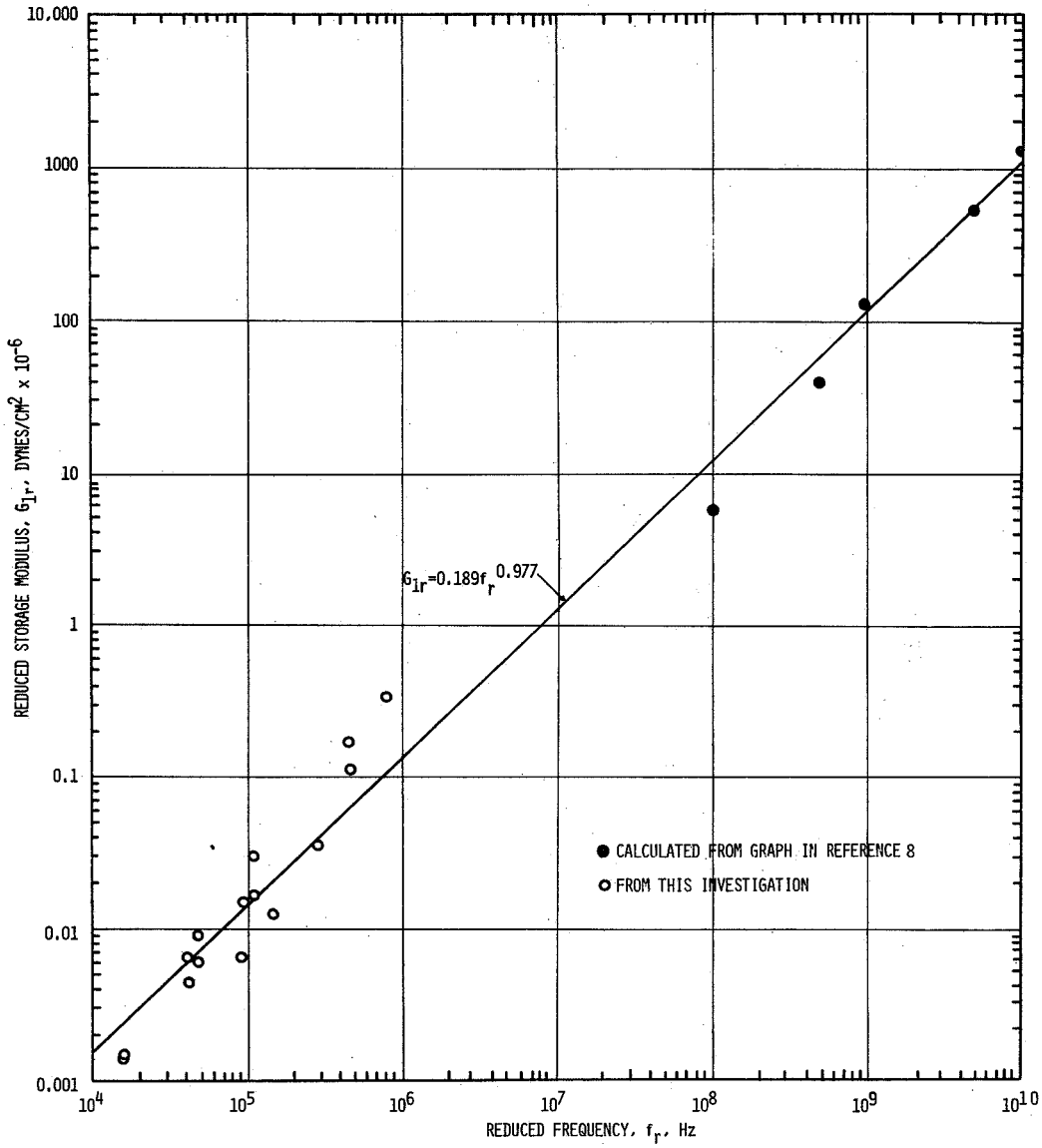

Figure 19. The Storage Modulus of di-(2-ethylhexyl) Sebacate.

Furthermore, this agreement serves as a confirmation of the concept of reduced variables.

The correlation shown in Figure 19 was used to calculate a shear relaxation spectrum for di-(2-ethylhexyl) sebacate by means of the defining Equation (7):

$$H \text{ (at } \tau = 1/\omega) = 2/\pi \text{ Im } G_{lr} \text{ (at } \omega e^{\pm i\pi/2}) \qquad (22)$$

where H is the relaxation spectrum

Im signifies the imaginary part of G_{lr} evaluated at $\omega e^{\pm i\pi/2}$.

This spectrum is shown in Figure 20; a relatively wide distribution of relaxation times is indicated.

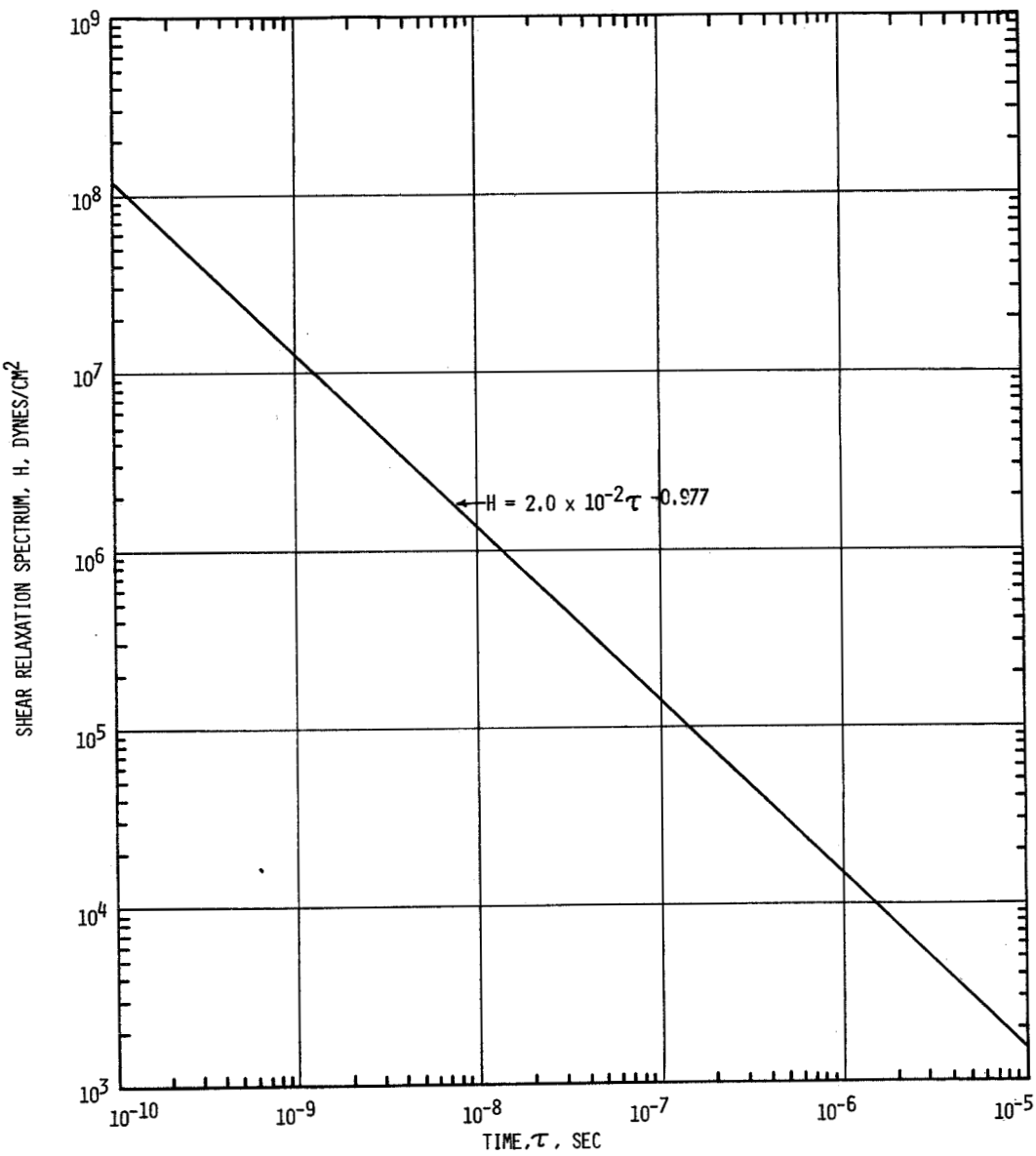

Figure 20. The Relaxation Spectrum of di-(2-ethylhexyl) Sebacate.

CONCLUSIONS

The principal conclusions resulting from this investigation are:

1. The present oscillating quartz crystal viscometer can be used to measure viscosities at elevated temperatures and pressures and discrete shear rates to an accuracy of at least ± 15 percent.
2. The concept of reduced variables in combination with viscosity measurements at high pressures to simulate high shear rates at atmospheric pressure has been reconfirmed.
3. Viscoelastic behavior is manifest at atmospheric pressure and 100°F for Mobil XRM-109 fluid at an angular frequency of about 5.9×10^5 radians per second and for Humble FN-3158 plus 10 volume percent Kendall 0839 at an angular frequency of about 4.7×10^6 radians per second.
4. Previous observations that the calibration parameters for the crystal viscometer, K_f and R_{Eo}, are independent of both pressure and temperature are confirmed. The dependency of the calibration parameter, f_o, on both pressure and temperature is also consistent with earlier studies. However, the observed change in the calibration parameter, K_r, with pressure has not been reported previously.
5. The viscoelastic behavior of one of the calibration fluids, di-(2-ethylhexyl) sebacate, as measured by the reduced elastic (storage) modulus, corresponds closely with data reported by Lamb in 1965 using a different technique. The calculated relaxation spectrum shows no maxima and is characteristic of a broad distribution in relaxation times.
6. A thorough investigation of the possible viscoelastic effects in fluids would require three experimental techniques: (1) The effect of pressure and temperature on viscosity at zero (or maybe very low) shear rates such as the falling-ball

method; (2) the effect of pressure, temperature and variable shear rates up to several million Hertz by the oscillating quartz crystal technique; and (3) the effect on viscosity of very high shear rates, at least up to 10^{10} Hertz by the quartz technique utilized by Barlow and Lamb.

LIMITATIONS AND REMEDIES

During this study several deficiencies in the design of the oscillating quartz crystal viscometer became evident which limited the range of feasible measurements. These shortcomings have since been corrected, or can be corrected, with a modest amount of development work. The fact that this particular equipment was entirely new and had not been used previous to the initiation of this study probably accounts for several of the experimental limitations uncovered during the earlier phases of the work. The major deficiency in the present design is the difficulty in handling very viscous fluids (10 poise) such as were encountered in this study.

Sensitivity

As the viscosity of the test fluid increases, the sensitivity of the measuring equipment decreases. The sensitivity, which is given by the ratio of the change in bridge output to the change in the resistance, is compromised as the resistance increases with increasing viscosity. For example, in this study it was very difficult to detect changes in resistances of less than 5 percent. Also, the dial on the bridge which indicates the resistance values has decreased resolution at the high end.

The limitation on dial resolution has been circumvented by inserting a 1.500 MΩ resistor in parallel with the crystal, thus lowering the measured resistance and thereby keeping the measured resistance within a readable range on the dial. This technique was used throughout the present investigation. Of course, this adaptation further reduced the sensitivity of the bridge output to crystal resistance changes, but the deleterious effect was more-than-compensated-for by the increased ability to read the dial. Also, with the parallel resistor, the actual

crystal resistance had to be calculated from the resistance relation for parallel resistors.

At present, further amplification of the bridge output signal, to increase measurement sensitivity effectively, is limited by noise associated with the signal. Decreasing the noise to permit greater amplification seems to be the most promising way to increase measurement sensitivity. Sources of noise, in order of decreasing probability of causing problems, are: (1) pickup by the leads from the crystal to the measuring equipment, (2) the oscillator and (3) mismounting of the crystal.

High Pressure Cell Design

In the present design, the test fluid is pressurized in the intensifier and is transferred into the high pressure cell containing the viscometer through a transfer line having an internal diameter of 0.025 inches. At higher pressures (above 40,000 psi) the viscous test fluids behave virtually as solids in the transfer line and it is not possible to pressurize the cell. Some preliminary attempts were made to heat the intensifier and transfer lines, but this remedy introduced more problems (with respect to the operation of the intensifier and the manganin coil) than it solved. The most promising solution is to enclose the crystal viscometer in a bellows. The test fluid would then be charged directly into the bellows chamber at essentially atmospheric pressure. It would then be brought to the desired pressure by using the intensifier and a low-viscosity fluid such as pentane to transmit pressure across the bellows to the test fluid. A schematic of this proposed design is shown in Figure 21. Another advantage for the bellows chamber is that it would reduce greatly the amount of test fluid needed for measurements.

Electrode Integrity

The silver electrodes on the quartz crystal are vacuum deposited. In the earlier stages of this investigation, it was observed that the silver tended to flake-off after pressurization

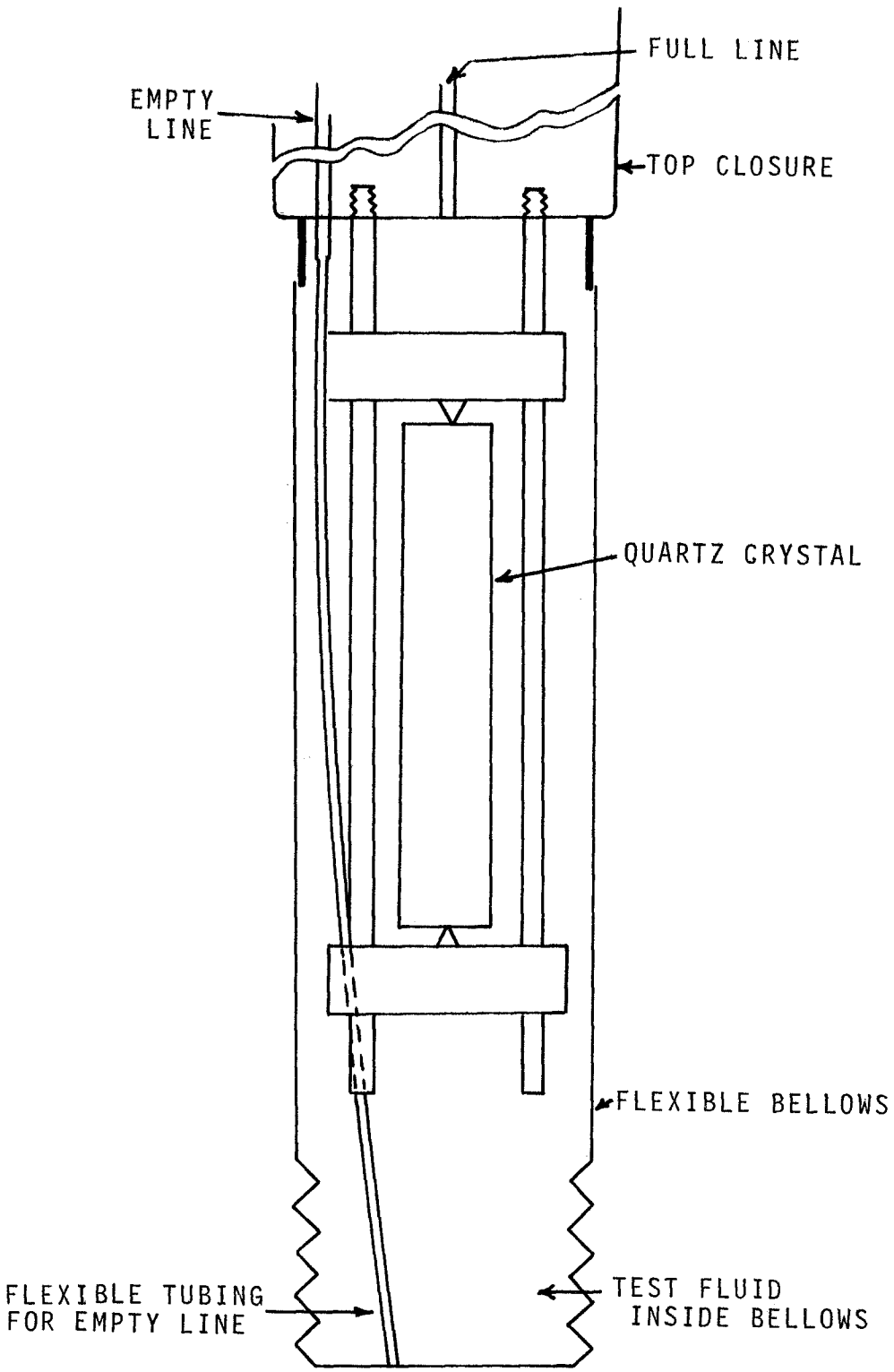

Figure 21. A Schematic Diagram of a Bellows Arrangement for Containing the Test Fluid in the High Pressure Cell.

at temperatures above 300°F, thus breaking the electrical circuit. This problem now appears to have been resolved by maintaining closer control of the thickness of the silver deposit.

RECOMMENDATIONS

1. The viscoelastic behavior of Mobil XRM-109 and the various mixtures of Humble FN-3158 with Kendall 0839 should be investigated further at higher pressures by the quartz crystal viscometer technique, particularly with a 100 kHz crystal. Although most of the measurements should be made at 100°F, for which viscoelastic behavior has been detected, measurements at higher temperatures would be desirable for conclusive confirmation of the data.
2. Additional measurements should be made on di-(2-ethylhexyl) sebacate at elevated pressures with the crystal viscometer to provide data for "filling-the-gap" in the relaxation spectrum between data from this investigation and a previous investigation.
3. The combination of the crystal viscometer and high pressure should be used for measurements on any fluid for which viscoelastic behavior is expected.

REFERENCES CITED

1. Appeldoorn, J. K., E. H. Okrent, and W. Philippoff, "Viscosity and Elasticity at High Pressures and High Shear Rates," Proc. Am. Pet. Inst., 42[III]:163, (1962).

2. ASME Pressure Viscosity Report, Volume II, (New York: The American Society of Mechanical Engineers, 1953).

3. Babb, S. E., Jr., "Simple High Pressure Valve," Rev. Sci. Instrum., 10:917, (1964).

4. Barlow, A. J., G. Harrison, J. Richter, H. Seguin, and J. Lamb, "Electrical Methods for the Viscoelastic Behavior of Liquids Under Cyclic Shearing Stress," Lab. Pract., 10:786, (1961).

5. Bridgman, P. W., "The Effect of Pressure on the Viscosity of Forty-Three Pure Liquids," Proc Am. Acad. Arts Sci., 61:57, (1926).

6. Bridgman, P. W., "The Volume of Eighteen Liquids as a Function of Pressure and Temperature," Proc. Am. Acad. Arts Sci., 66:185, (1931).

7. Ferry, J. D., Viscoelastic Properties of Polymers, (New York: Wiley, 1961).

8. Lamb, J., "Viscoelastic Behavior and the Lubricating Properties of Liquids," Symposium on Rheology, American Society of Mechanical Engineers, N. Y., 1965. See also, "The Viscoelastic Behavior of Lubricating Oils under Cyclic Shearing Stress," by A. J. Barlow, and J. Lamb in Proc. Roy. Soc. Series A, 253:62, (1959).

9. Loomis, W. R., NASA, personal communication, 1970.

10. Mason, W. P., "Measurement of the Viscosity and Shear Elasticity of Liquids by Means of a Torsionally Vibrating Crystal," Trans. Am. Soc. Mech. Eng., 69:359, (1949).

11. Philippoff, W., "Viscoelasticity of Polymer Solutions at High Pressures and Ultrasonic Frequencies," J. Appl. Phys., 34:1507, (1963).

12. Reid, R. C., and T. K. Sherwood, The Properties of Gases and Liquids, 2nd ed., Chap 3, (New York: McGraw-Hill, 1966).

13. Rein, R. G., Jr., C. M. Sliepcevich, S. E. Babb, Jr., and G. Tuma, "The Change in Resonant Frequency with Pressure to 8000 atm. of Quartz-Crystal Viscometers," J. Appl. Phys., 40:131, (1969).

14. Rein, R. G., Jr., Ph.D. Thesis, The University of Oklahoma, Norman, Oklahoma, 1967.

15. Rouse, P. E., Jr., E. D. Bailey, and J. A. Minkin, "Factors Affecting the Precision of Viscosity Measurements with the Torsion Crystal," Proc. Am. Pet. Inst., 30[III]:54, (1950).

APPENDIX A

TABULATED DENSITY DATA

APPENDIX A

TABULATION OF CALCULATED DENSITIES
AND PISTON DISPLACEMENTS

Fluid	Temperature (°F)	Pressure (1000 psi)	Displacement (in)	Density (gm/cc)
FN-3158	100*	atm	--	0.873
		10.0	6.500	0.905
		20.1	10.937	0.932
		39.8	17.812	0.970
	210*	atm	--	0.836
		10.0	7.312	0.872
		19.9	12.750	0.902
		40.4	20.375	0.945
	300*	atm	--	0.803
		10.0	9.000	0.846
		19.9	14.812	0.882
		39.5	22.812	0.925
	480	atm	--	0.739
		10.0	15.750	0.817
		19.9	23.625	0.858
		39.7	33.500	0.895
FN-3158+ 10 vol % 0839	100	atm	--	0.873
		9.8	7.125	0.905
		19.9	12.375	0.932
		38.2	19.500	0.970
	210	atm	--	0.836
		10.1	8.125	0.871
		20.0	13.937	0.902
		40.0	22.312	0.945
	300	atm	--	0.803
		9.9	9.875	0.846
		20.1	16.625	0.882
		40.0	25.250	
	482	atm	--	0.739
		10.0	17.375	0.817
		20.1	26.375	0.858

*Measurements at these temperatures were made using an oversize (0.660 dia.) piston. (Regular piston is 0.625 dia.)

APPENDIX A--Continued

Fluid	Temperature (°F)	Pressure (1000 psi)	Displacement (in)	Density (gm/cc)
XRM-109	100	atm	--	0.839
		10.0	7.250	0.871
		20.0	12.500	0.899
		36.3	18.825	0.937
	210	atm	--	0.806
		10.0	8.125	0.842
		20.0	14.187	0.872
	300	atm	--	0.778
		9.9	9.750	0.821
		19.8	16.438	0.855
Krytox	100	atm	--	1.88
		10.0	10.000	1.96
		19.9	16.375	2.04
		25.3	19.250	2.06
	210	atm	--	1.76
		10.2	12.750	1.88
		19.7	19.875	1.97
		28.0	24.125	2.02
	300	atm	--	1.67
		10.1	16.625	1.82
		19.9	24.750	1.92
		23.8	27.250	1.95
		26.4	28.500	1.96
	437	atm	--	1.50
		10.0	22.375	1.73
		19.9	32.000	1.87
		21.9	33.500	1.89

APPENDIX B

TABULATED VISCOSITY DATA

APPENDIX B

DATA FOR VISCOSITY CALCULATIONS AND CALCULATED VISCOSITIES

Fluid	Temp. (°F)	Press. (1000 psi)	R_E (kΩ)	R_M (gm/cm^2-sec)	f (Hz)	X_M (gm/cm^2-sec)	η_1 (p)	η_2 (dyne-sec/cm^2)
				60 kHz Crystal				
di-(2-ethylhexyl) sebacate	100	atm	281	150	62142.9	150	0.128	--
		4.94	344	187	62134.6	176	0.183	--
		5.17	347	188	62137.7	167	0.174	0.0215
		10.1	404	223	62129.5	192	0.233	0.0351
		18.0	524	300	62118.1	228	0.363	0.101
FN-3158	100	atm	649	347	62083.8	335	0.682	--
		4.92	967	525	62034.0	491	1.49	--
		9.94	1376	760	61943.6	773	3.34	--
		10.1	1333	736	61972.0	684	2.86	--
		18.1	2298	1313	61793.4	1242	9.08	--
FN-3158+ 10 vol % 0839	100	atm	741	396	62054.6	426	0.992	--
		5.3	1161	631	61999.9	597	2.17	--
		10.2	1641	907	61915.1	862	4.44	--
		18.4	2827	1615	61748.4	1383	12.4	1.94
XRM-109	100	atm	1489	796	61947.1	762	3.72	--
		2.24	1718	924	61917.8	854	4.78	--
		5.00	1736	943	61894.3	927	5.25	--
		9.64	2622	1449	61775.6	1298	11.1	1.22
Krytox	100	atm	1291	690	61963.3	712	1.35	--
		2.42	1721	925	61840.4	1092	2.74	--
		5.38	2324	1263	61714.7	1485	5.03	--
		9.80	3257	1799	61435.6	2358	11.2	--

APPENDIX B--Continued

Fluid	Temp. (°F)	Press. (1000 psi)	R_E (kΩ)	R_M (gm/cm^2-sec)	f (Hz)	X_M (gm/cm^{2}sec)	η_1 (p)	η_2 (dyne-sec/cm^2)
			20 kHz Crystal - II					
di-(2-ethylhexyl) sebacate	100	atm	378	78.7	19974.1	78.1	0.109	--
		10.2	585	135	19964.2	111	0.253	0.0507
		20.0	757	197	19954.9	145	0.471	0.145
		39.9	1507	411	19938.8	208	1.35	0.994
		60.0	2412	682	19932.4	252	2.64	3.09
	210	atm	212	43.5	19985.8	45.0	0.0363	--
		9.96	270	58.1	19981.3	63.1	0.0647	--
		19.7	358	88.5	19977.5	78.1	0.118	0.0146
		39.8	574	151	19969.1	119	0.293	0.0697
		60.2	787	216	19960.7	164	0.559	0.156
	300	atm	155	28.0	19989.2	35.0	0.0190	--
		10.2	216	45.0	19986.1	48.1	0.0392	--
		19.8	235	55.1	19983.2	59.4	0.0571	--
		40.4	345	87.3	19979.7	82.2	0.119	--
		59.7	448	119	19976.5	107	0.204	0.0225
FN-3158	100	atm	791	172	19949.0	157	0.656*	--
		10.0	1336	318	19897.9	318	1.79	--
	210	atm	290	58.8	19985.2	44.4	0.0497	0.0140
		10.2	433	100	19970.8	95.9	0.176	--
		20.1	568	145	19951.0	161	0.413	--
		39.9	977	263	19923.1	263	1.17	--
	300	atm	187	35.3	19988.7	36.6	0.0255	--
		10.2	258	55.1	19984.0	54.7	0.0567	--
		20.1	354	87.3	19977.9	75.9	0.138*	0.0168
		40.5	548	144	19957.4	152	0.377	--

APPENDIX B--Continued

Fluid	Temp. (°F)	Press. (1000 psi)	R_E (kΩ)	R_M (gm/cm^2-sec)	f (Hz)	X_M (gm/cm^2-sec)	η_1 (p)	η_2 (dyne-sec/cm^2)
				20 kHz Crystal - II				
FN-3158+ 10 vol % 0839	100	atm	1107	244	19938.6	189	0.845	0.219
	210	atm	383	79.9	19977.3	69.1	0.105	0.0153
		10.1	486	111	19970.1	98.1	0.199	0.0244
		20.0	714	185	19939.8	146	0.641	--
	300	atm	198	37.8	19987.2	41.3	0.0309	--
		10.1	297	64.6	19981.0	64.1	0.0779	--
		20.0	386	96.0	19972.2	93.8	0.163	--
		40.5	638	169	19942.7	198	0.577	--
XRM-109	100	atm	1894	423	19863.2	425	3.43	--
		10.2	3234	781	19806.2	604	8.71	2.26
	210	atm	505	108	19967.2	101	0.214	--
		9.86	767	179	19939.7	193	0.657	--
		20.0	1058	278	19892.0	345	1.76	--
	300	atm	281	56.6	19984.0	51.3	0.0594	--
		9.96	439	99.4	19974.0	85.9	0.092*	0.0243
		19.9	510	130	19952.8	154	0.373	--
		26.9	564	147	19948.8	169	0.455	--
		40.1	941	253	19916.3	280	1.26	--
				20 kHz Crystal - III				
di-(2-ethylhexyl) sebacate	100	atm	433	91.3	19968.0	81.7	0.132	0.0147
		9.96	670	152	19958.7	119	0.307	0.0759
		20.3	1069	273	19933.0	209	0.941	0.256
		39.9	2204	603	19875.3	416	3.99	1.52

APPENDIX B--Continued

Fluid	Temp. (°F)	Press. (1000 psi)	R_E (kΩ)	R_M (gm/cm^2-sec)	f (Hz)	X_M (gm/cm^2-sec)	η_1 (p)	η_2 (dyne-sec/cm^2)
				20 kHz Crystal - III				
di-(2-ethylhexyl) sebacate	210	atm	195	37.2	19982.6	38.0	0.0262	--
		10.0	282	59.6	19978.2	62.3	0.0655	--
		19.9	360	86.5	19976.1	76.0	0.112	0.0145
		40.2	550	144	19966.5	123	0.288	0.0458
		59.0	760	208	19954.2	185	0.605	0.0713
	300	atm	170	31.5	19985.3	32.3	0.0197	--
		9.96	196	39.1	19984.5	41.0	0.0290	--
		20.0	236	53.7	19980.0	65.3	0.0612	--
		40.3	336	84.4	19977.0	80.0	0.112	--
		58.6	439	116	19967.5	127	0.236	--

*These values calculated from $\eta_1 = \frac{2R_M^2}{\omega\rho}$ instead of $\frac{2R_M X_M}{\omega\rho}$ for reasons explained in the text, page 38 and 39.